Abstract

In Chapter I, the average pattern of the ionospheric current system of polar geomagnetic storms for the northern and southern polar regions is constructed by analyzing exactly simultaneous events during the IGY period. Those events are classified into two groups; *i. e.*, severe storms where $\overline{K}_p=7.4$ and moderate storms where $\overline{K}_p=4.3$. In both cases, the average D_p fields for northern and southern polar regions are almost exactly symmetric with each other with respect to the geomagnetic coordinates, suggesting that the geomagnetic linkage holds well between the two polar regions. Several remarks are made on the mechanism of causation of the D_p field. It is emphasized that the D_p field may comprise two components, namely, *SP*-component which is characterized by enhancement of the $S_q{}^p$ field by the stronger solar wind in storm time, and defined *AEJ*-component which has been known as the auroral electrojet concentrating along the narrow region of the auroral zone.

In Chapter II, similarity and simultaneity of geomagnetic bay type variations in geomagnetically conjugate areas in the northern and southern polar regions are discussed, based upon simultaneous data of individual bays. From the observed facts, it has been concluded that charged particles of nearly the same flux are precipitating simultaneously in the northern and southern polar ionospheres over the conjugate areas. Besides, it seems likely that nearly the same intensity of electric field is transferred to the both polar regions simultaneously from the magnetosphere. The conjugacy always holds well between the conjugate stations located in the auroral zone and the polar cap at the best-developed stage of geomagnetic bays. Some theoretical discussions are attempted on the structure of instantaneous and individual D_p field of geomagnetic bays.

In Chapter III, the conjugacy of storm sudden commencement (*SSC*) between conjugate points in the auroral zone is described based upon the simultaneous data observed at Syowa Station and Reykjavik. Similarity and simultaneity are good at the conjugate points for *SSC*s. Observed *SSC*s are elliptically polarized and the sense of rotation of polarization is counterclockwise and clockwise on the morning and afternoon sides respectively as viewed along the magnetic lines of force in both conjugate points. Comparing the characteristics of polarization and other morphological facts revealed by the present analysis with those of the $S_q{}^p$ field, it is concluded that the polar part of *SSC* is attributable

to the transfer of excess electric charge to the polar ionosphere from the outer magnetosphere, which is caused by fluctuation and enhancement of the $S_q{}^p$ field of a pre-*SSC* stage by the impact of storm time solar wind to the magnetosphere. The propagation of *SSC* seems to take the form of hydromagnetic wave propagation.

In Chapter IV, the conjugacy of sudden impulses (*SI*) between the conjugate stations in the auroral zone is described, using the simultaneous data obtained at Syowa Station and Reykjavik. Comparison of morphological characteristics of sudden impulse with those of storm sudden commencement indicates that *SI* and *SSC* are quite similar and sudden impulse may be caused by the same mechanism as that for *SSC*.

In Chapter V, the conjugacy of geomagnetic pulsations of several minutes in period (pc-5) between conjugate points in the auroral zone is discussed. Pc-5 pulsations have extremely good conjugate relations in regard to their time of occurrence and their wave forms. The polarization of the observed pc-5 is elliptic and the plane of polarization is approximately perpendicular to the geomagnetic lines of force. The sense of rotation of polarization vector is counterclockwise in the morning and clockwise in the afternoon as viewed along the magnetic lines of force. Therefore, pc-5 pulsation may be attributable to low frequency hydromagnetic wave generated in the outer magnetosphere and transmitted along the lines of force to both polar regions in the same manner.

CHAPTER I.
GEOMAGNETICALLY CONJUGATE RELATIONSHIP OF AVERAGE PATTERN OF POLAR MAGNETIC STORMS (D_p FIELD) DURING IGY PERIOD

I–1. Introduction

Geomagnetic phenomena observed in the polar region may be attributed to two different causes; one is the impinging charged particles on the ionosphere, and the other is the hydromagnetic motions propagating through the magnetospheric plasma.

Since the polar magnetic storms have been considered to be closely related to the transport phenomena of plasma particles to the ionosphere along the geomagnetic lines of forces from the quasi-steady radiation belt or some other sources in the magnetosphere, investigation of the geomagnetic conjugacy between the northern and southern polar regions seems very important in the sense of examining the manner of electromagnetic linkage between the two hemispheres through the magnetic lines of forces.

The main purpose of the present work is to demonstrate the ionospheric current systems of average D_p field of polar geomagnetic storms, using exactly simultaneous geomagnetic data observed in the northern and southern polar regions during the IGY period.

The geomagnetic coordinates adopted in all cases in the present work are not the ordinary geomagnetic coordinates but the corrected geomagnetic coordinates proposed by HAKURA (1964, 1965), so that the geometrical relationship between the northern and southern stations is referred very closely to the actual distribution of geomagnetic field.

The chief interest in this section is concerned with the average *DS* field within both polar regions which are higher than approximately 60° in geomagnetic latitude. Hence, the IGY magnetograms at 14 stations located between $\Phi_m=87.7°$ and $\Phi_m=56.3°$ and those at 9 stations between $\Phi_m=-87.7°$ and $\Phi_m=-50.0°$ are selected as the basic data. Locations of these IGY magnetic stations are listed in Table I–1. Magnetograms at these 22 magnetic stations for exactly the same time interval during storms are subject to analysis.

During the IGY period 28 typical magnetic storms were picked up. These

Table I-1. Location of magnetic stations whose magnetograms are used in the present analysis.

Northern polar region			Southern polar region		
Station	Correct. Geomag. Lat.	Correct. Geomag. Long.	Station	Correct. Geomag. Lat.	Correct. Geomag. Long.
Thule	87.7°	39.6°	Vostok	−87.9°	66.7°
Godhaven	77.6	43.3	Scott Base	−80.5	323.4
Murchison Bay	76.0	121.2	Wilkes	−79.7	157.6
Baker Lake	75.1	320.4	Mirny	−76.6	127.4
Chelyuskin	71.3	173.9	Little America	−74.3	332.8
Churchill	70.0	326.0	Byrd	−68.7	352.0
Dixson	68.0	154.9	Macquarie	−64.4	244.0
College	64.9	260.3	Halley Bay	−61.4	28.5
Cape Wellen	62.6	243.0	Amberley	−50.0	253.6
Sitka	59.8	276.6			
Lerwick	58.9	84.3			
Srednikan	56.3	217.7			

Table I-2. Data and time of occurrence of commencements of magnetic storms analyzed in the present work.

Severe Storm					Moderate storm				
Year	Month	Date	Time	Max k_p	Year	Month	Date	Time	Max k_p
1958	March	11	23^h 16^m	7_0	1958	Jan.	25	10^h 50^m	4_+
〃	May	31	16 52	8_0	〃	Feb.	4	13 04	4_+
〃	June	7	0 46	8_-	〃	March	3	9 31	4_-
〃	〃	28	17 42	8_0	〃	〃	17	7 50	5_0
〃	July	8	7 48	8_-	〃	〃	31	4 21	4_+
〃	Aug.	17	6 52	7_+	〃	April	26	12 47	5_-
〃	〃	22	2 47	6_-	〃	June	8	17 28	4_+
〃	〃	24	1 40	8_-	〃	〃	14	18 28	5_0
〃	〃	27	2 43	7_-	〃	〃	21	2 06	5_-
〃	Sept.	3	8 43	7_-	〃	Sept.	30	10 05	4_-
〃	〃	4	13 39	9_-	〃	Nov.	28	1 09	4_0
〃	〃	25	4 8	7_0	〃	Dec..	4	0 35	4_+
〃	Oct.	24	7 31	7_+	〃	〃	13	0 01	5_+
〃	Dec.	17	18 17	7_0	〃	〃	15	20 22	3_+

storms are classified into two groups, *i. e.* group of severe storms and that of moderate ones, according to the magnitude of their maximum K_p values; that is, a storm with the maximum K_p greater than 6 is classified as a severe storm, and that with the maximum K_p smaller than 5 is defined as a moderate storm.

Table I–2 shows the data and times of sudden commencements of 14 severe storms and 14 moderate storms which are referred to the list of geomagnetic and solar data in the Journal of Geophysical Research and also to the storm list of the I.A.G.A. monograph. The K_p values at each maximum stage of individual storms are also indicated.

In their studies of disturbance field, NAGATA and FUKUSHIMA (1952, 1954) interpreted the geomagnetic disturbance field D as an addition of the polar disturbance field D_p and the non-polar component D_z which is attributable to the magnetic field by the idealized ring current in the magnetosphere, namely, $D=D_p+D_z$.

A similar interpretation has been presented by CHAPMAN (1962) who considered the disturbance field is the superposition of the polar substorm D_p, the field caused by the solar corpuscular stream, DCF, and the field produced by the ring current, DR, namely, $D=DP+DCF+DR$. CHAPMAN's DP is identical with NAGATA-FUKUSHMA's D_p.

It has been well known that the development and decline of the D_p field of a storm is closely connected with increase and decrease of the D_{st} field of the storm (NAGATA and ONO, 1952; SUGIURA and CHAPMAN, 1960). According to NAGATA and ONO, the polar DS field on average is in its maximum-developed stage from about 4^h to 12^h in storm time. SUGIURA and CHAPMAN presented the rates of evolution of the DS field at middle latitudes in comparison with those of the D_{st} field, indicating that the DS field is in the best-developed stage from about 3^h to 10^h in storm time.

As for the D_{st} field in low latitudes, SUGIURA has proposed the most reasonable expression of equatorial D_{st} and has published tables of hourly values of equatorial D_{st} for the IGY, using the hourly D values obtained at longitudinally well distributed stations between 10° and 30° in geomagnetic latitudes.

According to this result, D_{st} of the storms in IGY are divided roughly into two groups by their D_{st} patterns; one is with short ($\leqq 1$ hour) initial phase and large main phase ($D_{st} \gtrsim 100\gamma$), and the other is with long initial phase (>1 hour) and small main phase ($D_{st} < 100\gamma$).

Taking the above-mentioned facts into consideration, the geomagnetic disturbances of the best-developed 6 hours in the main phase of SUGIURA's D_{st} are used in the present analysis. The average K_p indices during the most active 6 hours for 14 severe storms and 14 moderate storms are $\overline{K_p}=7.4$ and $\overline{K_p}=4.3$, respectively.

I–2. Simultaneous current patterns of the average D_p field in the northern and southern polar regions

With regard to the local geomagnetic time, readings of every 30 minutes of geomagnetic disturbances observed at 22 polar magnetic stations during the most active six hours of individual storms are averaged separately for severe and moderate storms. The average disturbances thus obtained are plotted in the coordinates of the corrected geomagnetic latitudes and longitudes (HAKURA, 1965) separately for the northern and southern polar regions.

The geomagnetic disturbances are defined as the deviations from the geomagnetic values just before the commencement of the storms. Since only the most active stages of polar magnetic storms are dealt with in the present work, the above-mentioned approximate definition of the base line value for disturbances would involve practically no serious error.

In the process of determining the equivalent current system, the horizontal components ΔH and $H\Delta D$ are mainly used, while the vertical disturbances are referred only as supplementary data. It is assumed as usual that two-third of the horizontal disturbances are due to the overhead ionospheric currents.

Denoting the horizontal force of equatorial D_{st} value by H_e, the horizontal force H of D_{st} at any geomagnetic latitude Φ_m may be approximately expressed as

$$H = H_e \cos \Phi_m.$$

Based on the values in SUGIURA's table, average values of H_e are computed in a similar way to that for computing the polar D_p distribution. Namely, the average H_e of individual storms is defined as the average deviation of H_e values during 6 hours corresponding to the time interval used for determining the D_p of the individual storm.

The average values of H_e thus obtained for 14 severe storms and 14 moderate storms are -120γ and -10γ, respectively. According to the definition, the D_z component is represented by the zonal current around the geomagnetic axis. Substracting the average D_z field from the average D field thus obtained the D_p field in both polar regions is obtained.

Fig. 1-1 and Fig. 1-2 illustrate respectively the average D_p field current systems in the northern and southern polar regions for the severe and moderate

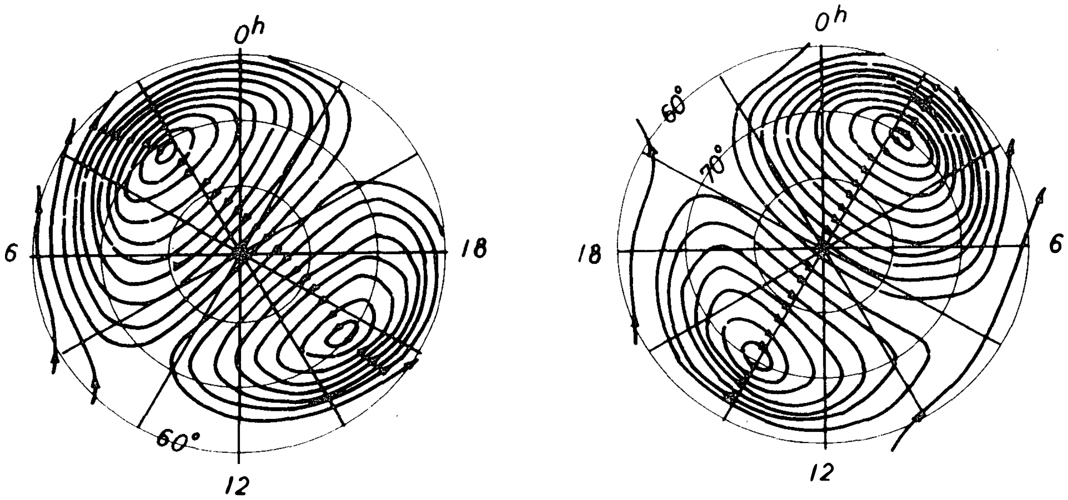

Fig. 1-1. Ionospheric current pattern of D_p field for average severe storm ($\overline{K}_p=7.4$) in the northern (left) and southern (right) polar regions. Electric current between adjacent current lines is 5×10^4 amperes.

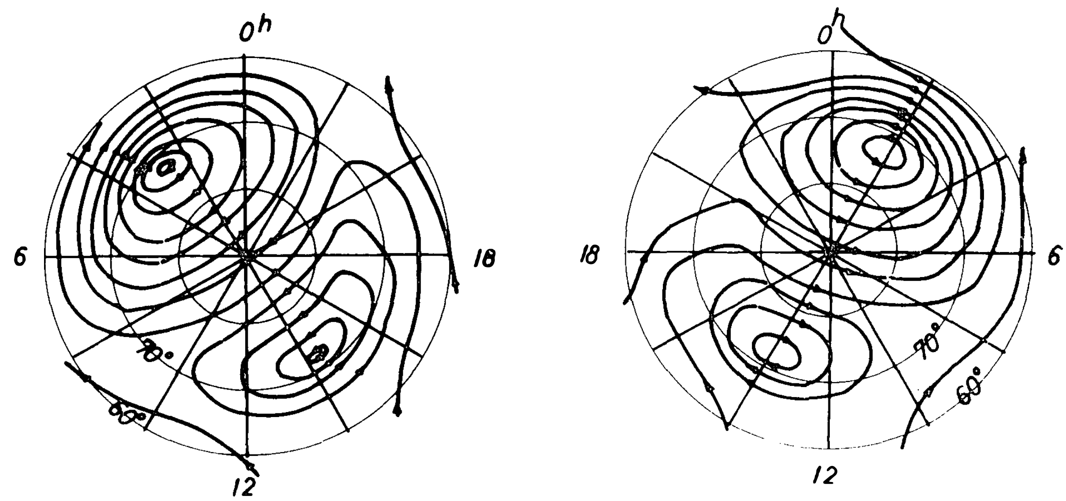

Fig. 1-2. Ionospheric current pattern of D_p field for average moderate storm ($\overline{K}_p=4.3$) in the northern (left) and southern (right) polar regions. Electric current between adjacent current lines is 5×10^4 ampere.

storms. The electric current flowing the adjacent line in these four diagrams is 5×10^4 ampere. All these figures indicate that the southern patterns of the D_p field are substantially the same as the simultaneous northern patterns in both cases of the severe and moderate storms, the former being in good conjugate relationship with the latter with respect to the corrected geomagnetic coordinates. The amount of the total current in the polar cap is about 85×10^4 amp and 45×10^4 amp respectively for the severe ($\overline{K}_p=7.4$) and moderate ($\overline{K}_p=4.3$) storms.

In the case of an average storm, the current intensity of the westward auroral electrojet is about 40×10^4 amp on the midnight-morning side and about 30×10^4 amp on the day-evening side of the eastward electrojet. The ratio of the auroral zone D_p field to the polar cap D_p field is 3.0 and 2.2 for the westward and eastward electrojets respectively.

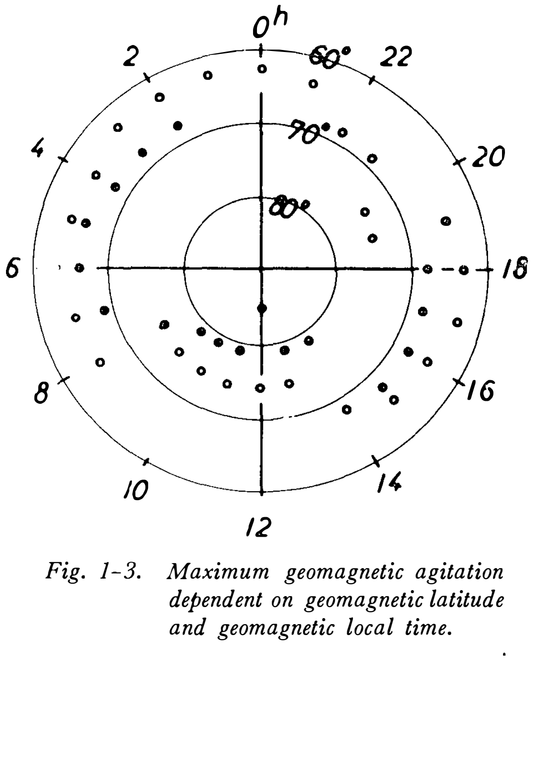

Fig. 1-3. Maximum geomagnetic agitation dependent on geomagnetic latitude and geomagnetic local time.

The current intensity of the electrojet in the case of moderate storms is about 25×10^4 amp and 10×10^4 amp respectively for the midnight-morning side and the daytime-evening side of the auroral zone. The rate of the intensification of the magnetic disturbances in the auroral zone is 2.8 and 1.8 respectively for the westward and eastward electrojets. Therefore, the intensification of the auroral electrojet as compared with the polar cap current is a little larger in severe storms than in moderate ones.

The spiral pattern, which is defined in this work as the locus of the points where the largest magnetic disturbances are observed on each geomagnetic latitude circle, was also studied using the data of 22 magnetic stations listed in Table I-1. The result is shown in Fig. 1-3.

The conjugacy of the current intensities and the geometrics of the current patterns are summarized as follows:

Severe storm ($\overline{K_p}=7.4$)

	Northern polar region	Southern polar region
Direction	9^h	9^h
Current vorticies		
morning side	70°, 2.2^h	70°, 2.2^h
afternoon side	71°, 15.7^h	71°, 14.3^h
Intensity		
polar cap	85×10^4 amp	85×10^4 amp
westward *AEJ*	40×10^4 amp	35×10^4 amp
eastward *AEJ*	30×10^4 amp	25×10^4 amp

Moderate storm ($K_p=4.3$)

	Northern polar region	Southern polar region
Direction	9^h	8^h
Current vorticies		
morning side	72°, 2.5^h	72°, 2.4^h
afternoon side	72°, 14.4^h	72°, 13.9^h
Intensity		
polar cap	45×10^4 amp	45×10^4 amp
westward *AEJ*	25×10^4 amp	20×10^4 amp
eastward *AEJ*	10×10^4 amp	10×10^4 amp

I-3. Structure of polar magnetic storms

It has been concluded (NAGATA and KOKUBUN, 1962) that the polar regions of the earth are subject to an additional geomagnetic daily variation field *i. e.* S_q^p field, even on geomagnetically calm days, and that the current patterns of the S_q^p field are quite similar to the polar cap part of the D_p field, consisting of two current vorticies.

Then it may be reasonably considered that the D_p field is attributed to (a) strengthening of polar cap current system of the S_q^p field, and (b) enhancement of the auroral zone current developed by the auroral electrojet. From now on, the former is noted as *SP* and the latter as *AEJ*. Thus, D_p may be composed of SP and AEJ-components and expressed as

$$D_p = SP + AEJ.$$

The total amount of polar cap current of the $S_q{}^p$ field is about 1.5×10^5 amp in the sunlit polar cap and about 0.5×10^5 amp in the dark polar cap, the mean value being about 1.0×10^5 amp when $K_p=1.1$ for the calm period (NAGATA and KOKUBUN, 1962.) On the other hand, the total amount of polar cap current of the D_p field obtained in the present work is about 8.5×10^5 amp and 4.5×10^5 amp for the severe ($\overline{K_p}=7.4$) and moderate ($\overline{K_p}=4.3$) storms respectively.

Further studies have been made on the polar cap current of geomagnetic bays whose average K_p values are between 2 and 3. In the northern polar region, the total current of the D_p field of geomagnetic bays (D_p (B)) is about 2.3×10^5 amp for the sunlit condition ($\overline{K_p}=2.4$ for 24 bays) and about 1.5×10^5 amp for the dark condition ($\overline{K_p}=2.8$ for 17 bays), the average being 1.9×10^5 amp. It may thus become obvious that the polar cap current system consisting of two current vortices increases its intensity with increasing geomagnetic activity represented by the average K_p value.

As for the origin of the $S_q{}^p$ field, NAGATA and KOKUBUN proposed that the electric charges, which are produced in the magnetosphere by twisting of the geomagnetic lines of force owing to the hydromagnetically viscous-like interaction between the solar wind and the geomagnetic field, are transferred through the magnetosheric plasma along the lines of force to the polar ionosphere, producing the Hall current which is responsible for the $S_q{}^p$ field.

The linear speed of distortion of the lines of force near the magnetopause is estimated at about 3 km/sec for the $S_q{}^p$ field. Remembering that the $S_q{}^p$ field takes place even under the $\overline{K_p}=0$ condition, it may be approximately stated that the velocity of magnetospheric plasma near the magnetopause 3 km/sec, (assuming that the magnetospheric plasma is the medium density plasma in which the mean free path of plasma is much larger than the electron gyration radius and that the electrical potential difference along the geomagnetic line of force becomes negligible), is derived from the solar wind of about 300 km/sec in velocity under calm condition. An increase in the K_p value represents an increase in the solar wind velocity (SNYDER, NEUGEBAUER and RAO, 1963). The faster speed of the solar wind may result in the faster speed of the circulation of low energy magnetospheric plasma and consequently the larger electric current flow in the polar ionosphere, which may greatly contribute to the enhancement of $S_q{}^p$, *i. e.* SP-component of the D_p field, although the detailed mechanism of transformation of momentum from the solar wind into the magnetospheric plasma through magnetopause has not been clarified yet.

In addition to the polar cap current system consisting of two vortices, the auroral electrojets are definitely developed in the D_p field, particularly in the case of severe storms. Since the $S_q{}^p$ field has no enhancement of electric currents in the auroral zone, the auroral electrojet is a characteristic aspect of the D_p field.

It has already been established that in individual cases the auroral electrojet is accompanied by high ionization of the ionospheric E region and auroral displays (OGUTI and NAGATA, 1961). The observed ionization is high enough to multiply the electric conductivity of the lower part of the ionosphere by 10^1-10^2 or more. Then, the concentration of the large increase in the ionospheric conductivity in the auroral zone may result in the formation of the auroral electrojet.

In addition to this, the auroral electrojet must be driven by some other energy sources located in the ionosphere and in the magnetosphere. As an ionospheric source, the wind in the upper atmosphere has been assumed to drive the ionospheric current, as exemplified in the dynamo theory (NAGATA and FUKUSHIMA, 1951, 2; COLE 1960, 2; SWIFT, 1963).

When the dynamo theory is applied to the formation of auroral electrojet, it involves three difficulties; one is the phase difference between the observed ionospheric wind system and the theoretically required wind system for driving the auroral electrojet; the second is that the theoretical ratio of the intensity of auroral jet to that of S_q current is appreciably smaller than the observed value owing to the polarization effect on the auroral inhomogeneous ionization; the third difficulty is that the theoretically required ionospheric wind velocity is much larger than observed one.

Moreover, the transfer of the polarization electric field produced in the ionosphere to the magnetosphere and the ionospheric magnetospheric coupling through magnetic lines of force are neglected. In spite of the above-mentioned difficulties, the dynamo mechanism may account for a part of the auroral electrojet.

Another possibility of driving the auroral zone electrojet has been proposed. The *AEJ* currents may be driven by the electric field produced by the interaction of the solar wind and the magnetosphere. The electric field is transferred to the lower ionosphere through highly conductive magnetic lines of forces, currents flowing along the magnetic lines of forces. AXFORD and HINES (1961), FEJER (1963, 4), VESTINE and KERN (1962) and CHAMBERLAIN (1962) have assumed that the magnetospheric plasma is the medium density plasma with essentially no electric potential difference along the magnetic lines of force, and that the applied electric field responsible for the observed auroral electrojet is essentially the Hall current perpendicular to the auroral zone. The electric field is assumed to be driven by charge accumulation or charge separation in the magnetosphere by the relative motion between the low energy and high energy plasmas or by the magnetic field gradient in the magnetosphere.

The effective electric field which is the sum of the electric field supplied from the magnetosphere and the polarization field produced in the highly conductive area in the auroral zone is not simply proportional to the applied electric field. The rate of intensification of the ionospheric current depends largely on the shape of the auroral activated area rather than on the intensity of the applied electric field transverse to the auroral zone, provided $k \geqq 10$ (NAGATA and FUKUSHIMA, 1952), where k denotes the rate of intensification of the ionospheric conductivity. As seen from the current systems of the D_p field of severe and moderate storms, the region of auroral electrojet is a narrow band in shape and the ratio of its length to its width is more than 20. Thus, in the highly conductive auroral zone, the longitudinal electric field seems more effective than the transverse electric field which has been proposed in the charge separation mechanism by KERN (1961) and CHAMBERLAIN (1961).

On the other hand, ALFVÉN, FÄLTHAMMAR and BOSTRÖM (1964) have proposed an auroral jet theory by considering the magnetosphere as the low density plasma in which the current flow between the magnetosphere and the ionosphere is limited.

It may be tentatively concluded that the D_p field of polar magnetic storms is composed of two parts. One part is the defined *SP*-component attributable to an enhancement of $S_q{}^p$, which may be caused by the ionospheric Hall currents whose electric field is produced by the stronger motion of the low energy plasma through the viscous-like coupling between the storm-time solar wind and the geomagnetic fields and transferred to the lower ionosphere along the extremely conductive geomagnetic lines of forces.

The other part, which is characterized by the strongly intense current along the narrow region of the auroral zone and is called the *AEJ*-component, may be caused by at least two mechanisms; the anomalous increase of ionospheric conductivity by the impinging charged particles along the magnetic lines of force from some sources in the magnetosphere and the electric field driven in the magnetosphere by some mechanism, in which the charge separation mechanism may be partially effective.

CHAPTER II.
CONJUGATE RELATIONSHIP OF INDIVIDUAL GEOMAGNETIC BAYS BETWEEN THE NORTHERN AND SOUTHERN POLAR REGIONS

II–1. Introduction

It has been concluded based on the simultaneous average D_p field that the two polar regions of the earth are magnetically disturbed almost equally and in the same manner, on average. The patterns of the average D_p field with respect to the corrected geomagnetic latitude and geomagnetic local time in the north polar region are almost identical with those in the south polar region. In order to deal with some more details of the onset, development and decline of magnetic disturbances in both polar regions, in relation to possible physical mechanism of these disturbances, further studies on the time dependent characteristics of the conjugate relationship of individual D_p fields will be required. As the best existing pair of geomagnetically conjugate stations is the couple of Syowa Station ($\Phi_m=-66.7°$, $\Lambda_m=72.5°$) in Antarctica and Reykjavik ($\Phi_m=66.7°$, $\Lambda_m=71.2°$) in Iceland, the simultaneous magnetograms for individual geomagnetic bays observed at the two stations will be examined in some details with respect to their time variation. Then, the conjugacy of equivalent current patterns of some individual bays between the northern and southern polar regions will be examined as time sequences.

II–2. Similarity and simultaneity of geomagnetic bays at Syowa Station and Reykjavik

Eight examples of simultaneous geomagnetic bays observed at the Syowa Station and Reykjavik are shown in Fig. 2–1.

(a) Negative bay on May 15, 1959

This example (Fig. 2–1(a)) shows a sharp negative bay occurring at about 0^h in local geomagnetic time at both the conjugate stations. At these two points, bays attain their maximum stage almost simultaneously at 02^h40^m with the amplitude about 250γ. H-components are similar and in-phase at the conjugate points,

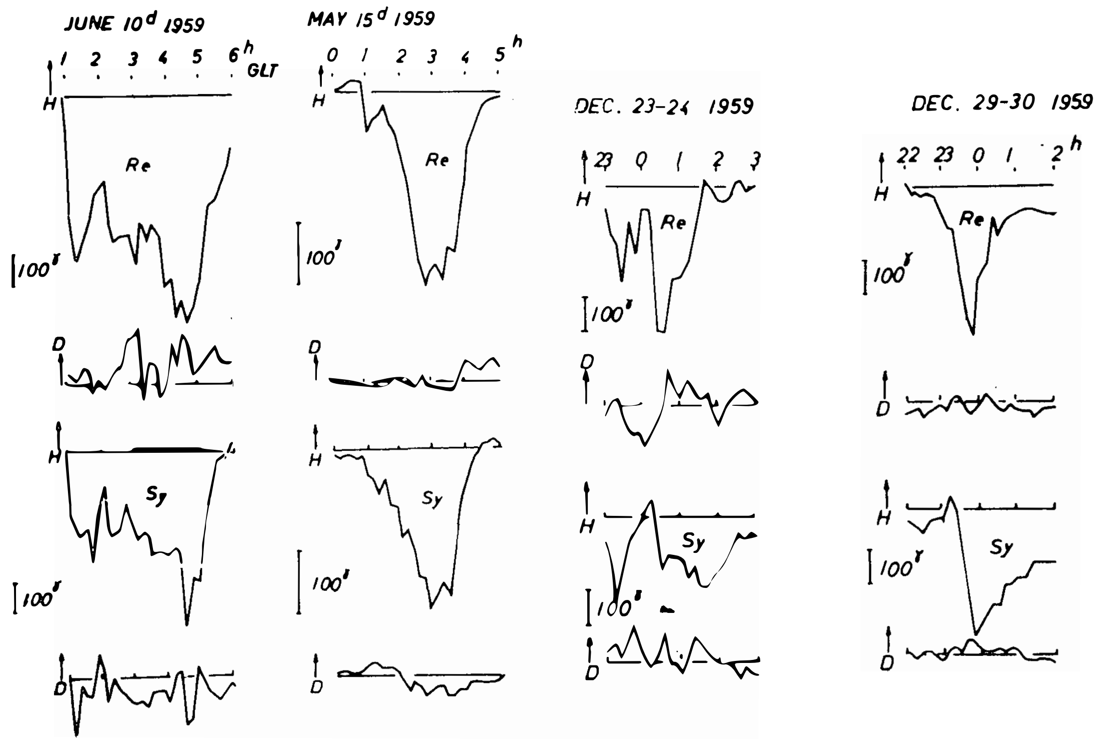

(a) (b)

Fig. 2-1. Examples of negative bays observed simultaneously at Syowa Station (Sy) and Reykjavik (Re).

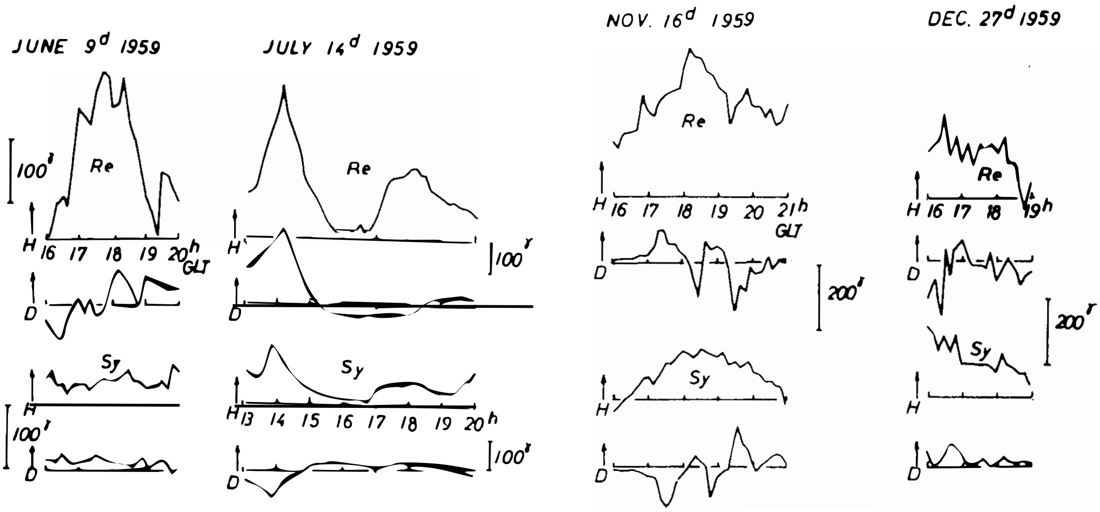

(c) (d)

Fig. 2-1. Examples of positive bays observed simultaneously at Syowa Station (Sy) and Reykjavik (Re).

and D-components are symmetric about geomagnetic coordinates and anti-phase with each other. The correlation coefficient of this example is 0.95, suggesting an extremely good conjugacy.

(b) Positive bay on July 14, 1959

Fig. 2-1(c) shows a so-called broad positive bay occurring almost simultaneously at 13^h in geomagnetic local time. As in the case of negative bay, H-components of this positive bay are similar and in-phase, but D-components are out-of-phase at conjugate points. The correlation coefficient amounts to 0.65 and is smaller than in the case of negative bay. H-component of Reykjavik is about three times larger than that of Syowa Station.

In another positive bay on Nov. 16, 1959 (Fig. 2-1(d)), which occurred nearly in the winter solstice at Syowa Station, the amplitude at Reykjavik is also three times as large as that of Syowa Station. This inequality of amplitude is observed in every case of examined 9 positive bays. The amplitude at Reykjavik is always

Table II-1(a). Correlation coefficient for negative bays.

Year	Month	Date	Onset time	Duration	Coefficient
1959	May	15	0^h 50^m	4^h	0.95
〃	〃	24/25	21 10	3	0.62
〃	June	10	1 00	5	0.82
〃	〃	20	0 20	4	0.90
〃	Sept.	5/6	21 10	5	0.77
〃	〃	8/9	22 30	3	0.95
〃	〃	13/14	21 30	4	0.88
〃	〃	17/18	20 00	4	0.80
〃	Nov.	6	0 30	6.5	0.84
〃	〃	20	0 00	3	0.83
〃	〃	24	11 00	3	0.94
〃	Dec.	23/24	22 00	2.5	0.52
〃	〃	27/28	22 30	4	0.79
〃	〃	29/30	22 00	4	0.79

Table II-1(b). Correlation coefficient for positive bays.

Year	Month	Date	Onset time	Duration	Coefficient
1959	May	14	12^h 40^m	6^h	0.74
〃	〃	24	12 30	6	0.63
〃	July	14	12 50	7	0.65
〃	June	9	16 00	4.5	0.60
〃	Sept.	5	16 00	4.5	0.64
〃	Nov.	16	16 30	4	0.47
〃	Dec.	27	15 30	3	0.56

larger than at Syowa Station regadless of seasons.

The correlation between H traces of 14 negative bays and 9 positive bays observed at Syowa Station and Reykjavik are calculated with regard to every five and ten minutes readings, the obtained correlation coefficients being summarized in Table II-1.

The correlation coefficient for negative bay ranges from 0.52 to 0.95, the average value being 0.81, whereas the coefficient for positive bays varies from 0.47 to 0.74, the average value being 0.61. Two examples of correlation diagrams for each positive and negative bays are illustrated in Fig. 2-2.

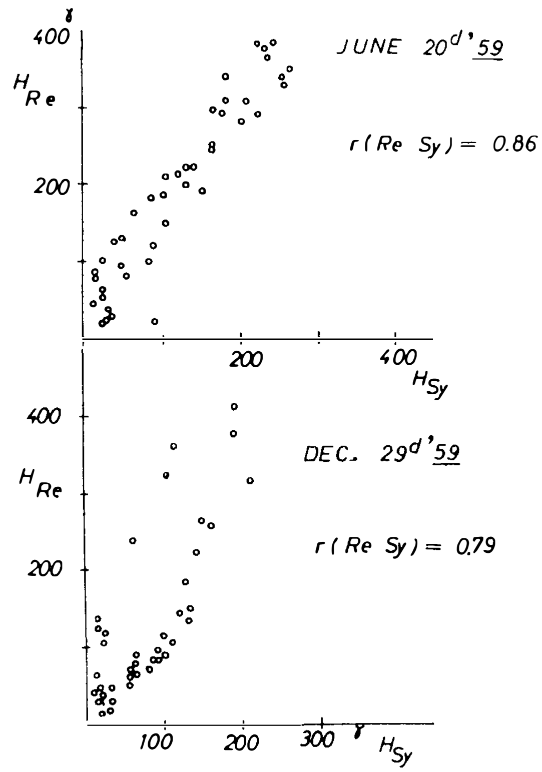

Fig. 2-2(a). Correlation diagram of deviation of negative bay between Syowa Station (H_{Sy}) and Reykjavik (H_{Re}).

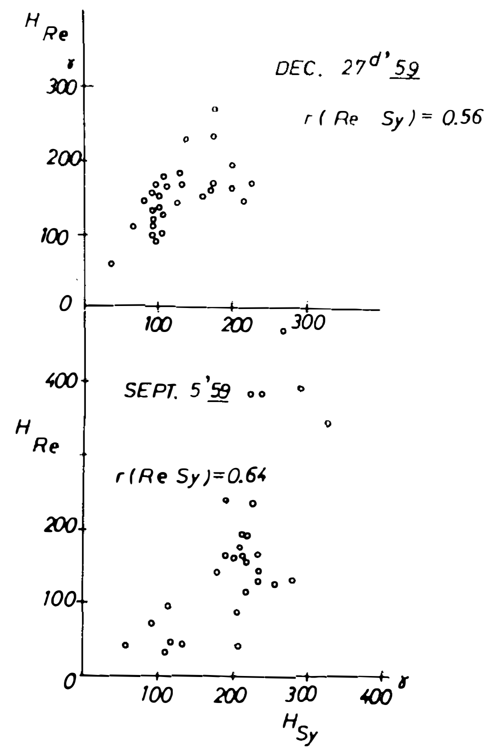

Fig. 2-2(b). Correlation diagram of deviation of positive bay between Syowa Station (H_{Sy}) and Reykjavik (H_{Re}).

Summarizing these statistical results, one may conclude as follows:

(1) At the conjugate points in the maximum auroral zones, Syowa Station and Reykjavik, both negative and positive bays occur almost simultaneously.

(2) The average correlation coefficient of 14 negative bays amounts to 0.86, which indicates a good conjugacy between the two points for negative bays.

(3) The average correlation coefficient of 9 positive bays which occur between 13^h and 20^h in geomagnetic time is 0.61. The positive bay has a little poorer conjugate relation as compared with the negative bay.

(4) As for the negative bays, the amplitudes of the horizontal components

are almost the same at the conjugate points. On the other hand, the positive bays at Reykjavik are always larger than those at Syowa Station independently of season.

More detailed examination of the time dependent conjugate relationship of the bays from the beginning to the declining stages has revealed that each peak of variation in individual bays does not always show one-to-one correspondence between the conjugate points.

Two examples will be dealt with for some detailed discussions:

(a) Negative bay on June 10, 1959

The correlation coefficient for this example amounts to 0.82. Therefore, the degree of conjugacy is fairly good in this case. Examining more precisely the records at the two conjugate points it is found that peaks appeared at $1^h\,20^m$, $2^h\,10^m$ and $3^h\,10^m$ quite simultaneously at the conjugate points. However, in the declining stage of the period of $4^h\,20^m$–$4^h\,50^m$, peaks and slots of H-components at the two stations are of out-of-phase with each other.

(b) Negative bay on Dec. 29–30, 1959

The correlation coefficient of the whole bay is 0.79. At the beginning stage of $22^h\,00^m$–$23^h\,20^m$ and the declining stage of $0^h\,20^m$–$1^h\,30^m$, variations of H-component of Syowa Station are not similar to those of Reykjavik.

It may be concluded, therefore, that the best-developed stage of the bay is generally in the best conjugate relationship, whereas the conjugacy is not always good in the beginning and declining stages of bays.

The spectral analysis may also be an appropriate method to examine the similarity of magnetograms between the conjugate stations. Fig. 2–3 illustrates two examples of spectrum of positive bays. In the case of a bay on July 14, 1959, the spectra at the two stations resemble each other, but the amplitude of spectrum at Reykjavik is markedly larger than that at Syowa Station, especially for larger periods. On December 27, 1959 also the spectrum has almost the same character at the two stations, but the amplitude of spectrum at Reykjavik is about twice as large as that at Syowa Station in spite of the condition that the former was

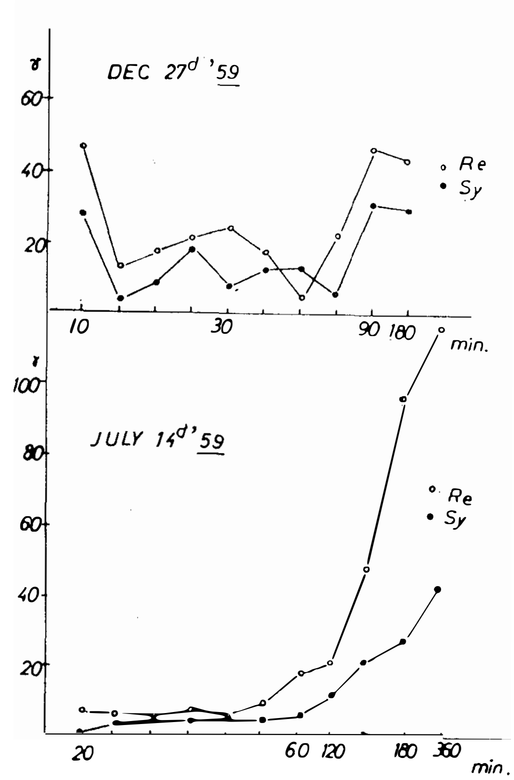

Fig. 2–3. Examples of period spectrum of geomagnetic bays observed simultaneously at Syowa Station (Sy) and Reykjavik (Re).

observed in winter and the latter in summer.

II–3. Geomagnetic conjugacy of equivalent current patterns of individual bays between the northren and southern polar regions

General features of geomagnetic conjugacy of equivalent current patterns of individual geomagnetic bays will be studied here, using the simultaneous data of individual events during the IGY period.

One full day magnetograms from Sept. 8, 20^h to Sept. 9, 20^h, 1958 is selected as a typical example and H, D, and Z components of 24 hour records are read evenry 10 minutes for 19 stations in the northern polar regions and 11 stations in the southern polar regions. These magnetograms include:

(1) Sharp negative bays during Sept. 8, 20^h – Sept. 9, 03^h in UT (Fig. 2–4),

(2) One large positive bay and one large broad negative bay during Sept. 9, 13^h – Sept. 9, 18^h in UT (Fig. 2–7).

As mentioned in the previous chapter, the D_p field seems to consist of two parts; *i. e.* an enhancement of $S_q{}^p$ and the auroral electrojet. From a detailed analysis of individual $S_q{}^p$ on Sept. 14, 1958 (an almost equinoctial day), $S_q{}^p$ seems to be divided into two components, *i.e.* a long period component, having the petiod longer than 6 hours, and another component with period shorter than 6 hours. Both components have nearly the same distribution pattern which is identical with the $S_q{}^p$ pattern proposed by NAGATA and KOKUBUN (1962). However, the short period component is rather sporadic and seems to be attributable to fluctuation of the average $S_q{}^p$ field. The longer period component is more than five times larger in amplitude than that of the short period component. Then, it may be said that the $S_q{}^p$ field always exists and the long period quasi-steady component, longer than 6 hours in period is dominant in the field.

As discussed in chapter I, the D_p field can be attributed partly to an enhancement of the $S_q{}^p$ field by a stronger solar wind; the SP-component of the D_p field may be attributable to the enhanced quasi-steady component of the longer period. The residual component of the shorter period of the D_p field will then be attributed mostly to the auroral electrojet.

In the present study, therefore, the D_p field is separated into the longer period component longer than 6 hours in period and the shorter period component shorter than 6 hours in period, using a numerical filtering method. The filtration was applied to three components of magnetograms obtained at 29 stations.

The results of such analyses are as follows:

(1) A sharp negative bay on Sept. 8, 20^h – 9, 3^h, 1958

This is a typical example of a sharp negative bay observed in the polar region during the period from pre-midnight (22^h) to post-midnight (03^h) in local geomagnetic time. As shown in Fig. 2–4, a negative bay was observed at Reykjavik, Kiruna, Cheluyskin, Dixson and Wellen which are located just in the geomagnetic local night time area in the northern polar region. At College, Meanook and Churchill which are in the local afternoon, on the contrary, small positive bays were observed. In the southern polar region also, a sharp negative bay was observed at the local night time stations such as Mawson and Macquarie Island. The area of occurrence of negative bay in this case was much wider than the area of positive bays at both northern and southern polar regions. The former was about 210° in geomagnetic longitude.

One-to-one correspondence of the geomagnetic bay between almost conjugate stations will be examined. At Thule and Vostok, which are located at 87.5° in geomagnetic latitude and differ from each other by about 2 hours in geomagnetic local time, *H*-components show almost similar patterns when the bay-disturbance attained to its maximum stage in the auroral stations. At the beginning stage of the first two hours (20^h-22^h in *UT*), the disturbance is much greater at Thule and the conjugacy was poorer than at the maximum stage.

In the middle polar cap region, Murchison Bay ($\Phi_m=76.0°$, $\Lambda_m=121.2°$) and Mirny ($\Phi_m=-76.6°$, $\Lambda_m=127.4°$) are fairly good conjugate points. At these points the disturbance patterns are not quite similar in the beginning two hours. When the bay attains to its maximum stage in the auroral zone, however, the conjugacy between these two stations became much better. At the declining stage the conjugacy becomes poorer again. In the auroral zone, Cape Wellen and Macquarie Island compose a comparably good conjugate pair. *H*-components at

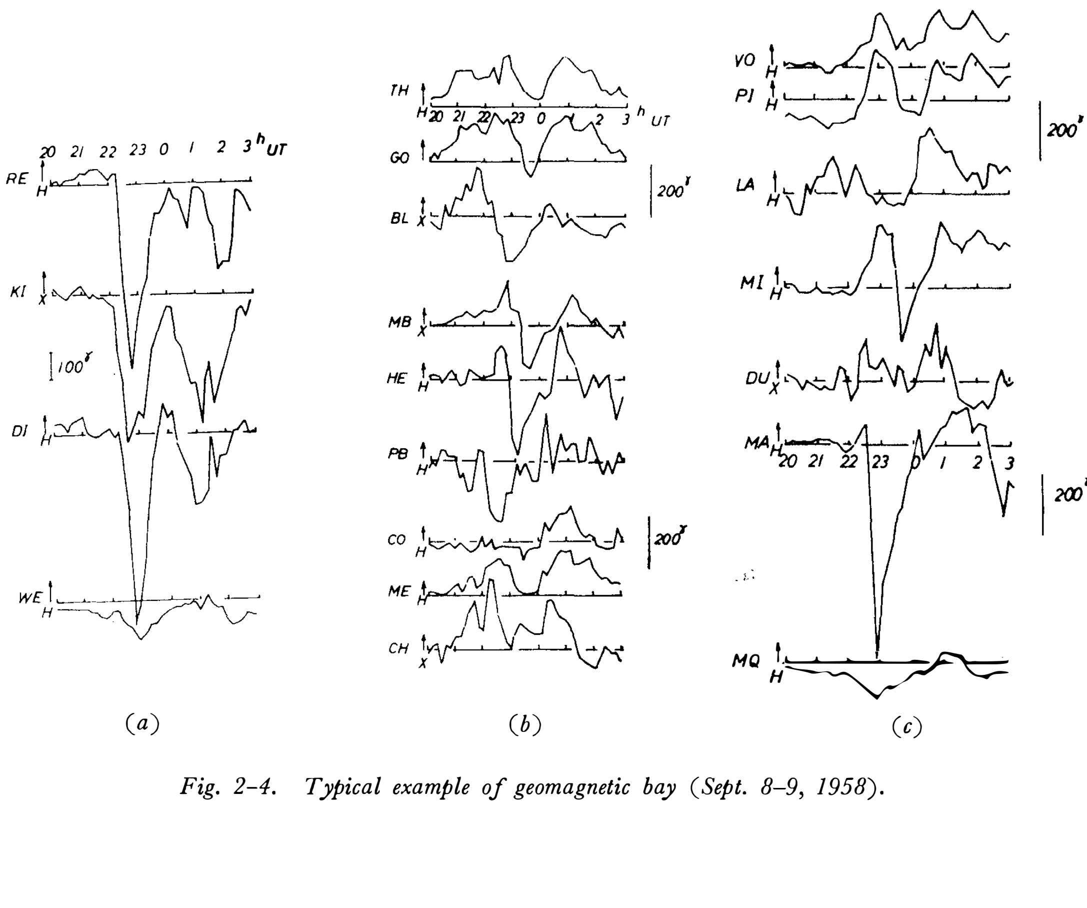

Fig. 2-4. Typical example of geomagnetic bay (Sept. 8–9, 1958).

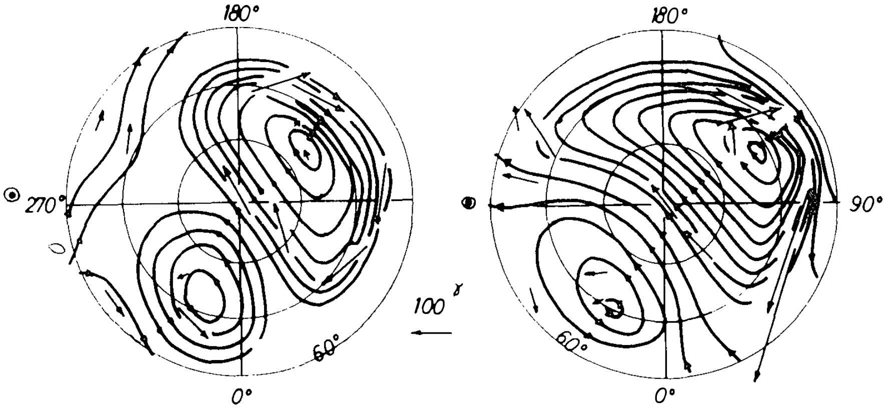

Fig. 2–5(a) Ionospheric current pattern of D_p field of instantaneous geomagnetic bay at 22^h 40^m; Sept.8, 1958 in the northern polar region.
Left: Long period component ($T_0 \geqq 6$ hours)
Right: Short period component ($T_0 < 6$ hours)
Current density: 5×10^4 amp.

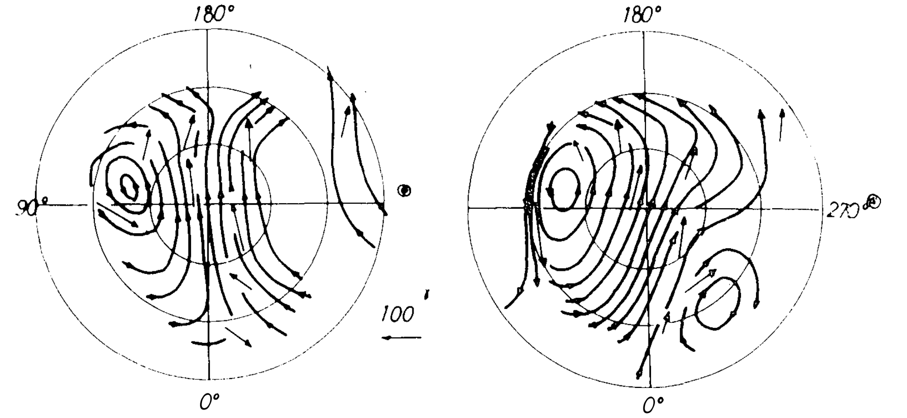

Fig. 2–5(b) Instantaneous D_p field on 22^h 40^m, Sept. 8, 1958 in the southern polar region.
Left: $T_0 \geqq 6$ hours.
Right: $T_0 < 6$ hours.

these stations are almost similar from the beginning to the end throughout the duration of the present bay. Since the auroral zone stations in the southern hemisphere are only three, the available data for the comparison of the bays are insufficient and unreliable.

Using the best-developed stages of this negative bay, which took place at 22^h 40^m and 1^h 40^m on the records of Reykjavik, Kiruna and Dixson in the northern polar region and of Mawson in the southern polar region, a general aspect of the distribution of disturbances is represented by the equivalent current patterns for the two components; *i. e.* the long period component ($T_0 \geqq 6$ hours) and the short period one ($T_0 < 6$ hours)(Figs. 2–5 and 2–6). For each component the geometries of the current patterns and current intensities are compared between the

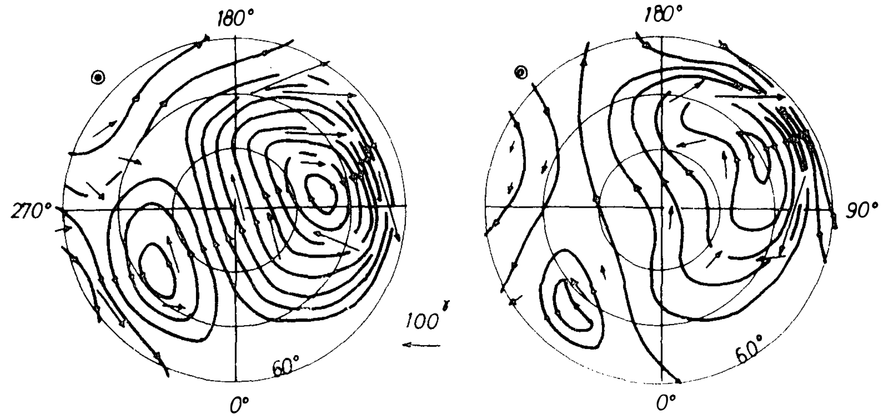

Fig. 2-6(a) Instantaneous D_p field on 01^h 40^m, Sept. 9, 1958 in the northern polar region.
Left: T_0 $\geqq 6$ hours.
Right: T_0 <6 hours.

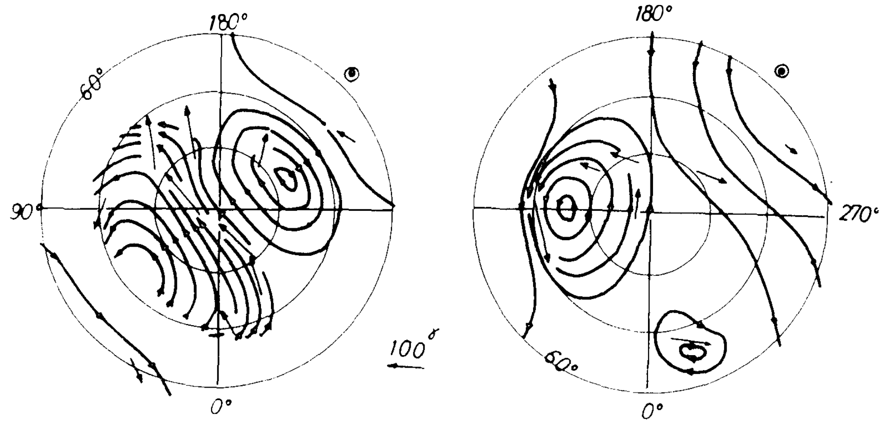

Fig. 2-6(b) Instantaneous D_p field on 01^h 40^m, Sept. 9, 1958 in the southern polar region.
Left: T_0 $\geqq 6$ hours.
Right: T_0 <6 hours.

two polar regions. Basic characteristics of the polar region currents of the D_p field are summarized in Table II-2.

Marked characteristics concluded from these tables will be as follows.

(i) At the best-developed stage of a sharp negative bay, the conjugacy holds well in both the polar caps and the auroral zones. The simultaneous current systems of the D_p field are symmetric with respect to the geomagnetic coordinates.

(ii) The intensity of the longer period component of D_p is almost the same in the two polar regions. The ratio of the auroral zone disturbance to the polar cap one is about 1.1 and 0.8 in the morning and afternoon auroral zones in the

Table II-2. Characteristic parameters of D_P field of sharp negative bays.

a. Long period component ($T_0 \geqq 6$ hours) at 22^h 40^m in UT (See Fig. 2-5).

	Northern polar region	Southern polar region
Direction	9^h	7^h
Current vorticies	73°, 17^h	—
	73°, 3^h	75°, 1^h
Intensity		
polar cap	143 amp/km	143 amp/km
auroral zone (a. m.)	166 amp/km	156 amp/km
auroral zone (p. m.)	125 amp/km	120 amp/km

b. Short period component ($T_0 < 6$ hours) at 22^h 40^m (See Fig. 2-5).

	Northern polar region	Southern polar region
Direction	10^h	9^h
Currence vorticies	72°, 2^h	73°, 2^h
	71°, 16^h	70°, 17^h
Intensity		
polar cap	112 amp/km	120 amp/km
auroral zone (a. m.)	387 amp/km (Φ_m=64.3°)	208 amp/km(Φ_m=−70.6°)
auroral zone (p. m.)	92 amp/km (Φ_m=69.0°)	—

c. Long period component at 01^h 40^m, Sept. 9th (See Fig. 2-6).

	Northern polar region	Southern polar region
Direction	10^h	7^h
Current vorticies	75°, 2.5^h	75°, 0^h
	74°, 17^h	76°, 13.5^h
Intensity		
polar cap	135 amp/km	150 amp/km
auroral zone (a. m.)	208 amp/km	—
auroral zone (p. m.)	114 amp/km	102 amp/km

d. Short period component at 01^h 40^m, Sept. 9th (See Fig. 2-6).

	Northern polar region	Southern polar region
Direction	10.5^h	9^h
Intensity		
polar cap	61 amp/km	71 amp/km
westward *AEJ*	306 amp/km (Φ_m=64.3°)	204 amp/km (Φ_m=−70.6°)
eastward *AEJ*	102 amp/km	—

northern polar region. In the southern hemisphere, the ratio is 1.1 for the morning and 0.8 for the afternoon for the best-developed stage (22^h 40^m UT). At 01^h 40^m, the ratio changes to 1.3 and 0.6 respectively for morning and afternoon auroral zones.

The current pattern of D_p consisting of two vortices is quite similar to that of $S_q{}^p$. The essential similarity between the longer period component SP of D_p and $S_q{}^p$ is that there is no definite auroral zone enhancement, suggesting that the SP field is due to an simple enhancement of the $S_q{}^p$ field.

(iii) The shorter period component is characterized particularly by the intense westward auroral electrojet on the night side of both northern and southern auroral zones. The intensity of these electrojets is about 3–5 times as large as that of the polar cap current. The eastward auroral zone current responsible for the positive bay is weak and is almost comparable with that of the polar cap current in the northern and southern afternoon auroral zones. This feature is similar to the D_p field of a sharp negative bay in the Second Polar Year obtained by NAGATA and FUKUSHIMA (1951, 1952). From these studies of individual and instantaneous D_p fields, it may be summarized that the longer and shorter period components seem to have their respective physical meanings, and the instantaneous D_p field can be considered to consist of an enhancement of $S_q{}^p$ and the auroral electrojet with its counter currents.

(iv) In the sharp negative bay discussed here, the D_p field attributable to the long period component is about 1.5–2.5 times larger than that which seems to be attributable to the long period component in the auroral zone in the northern and southern polar regions. It is likely that in the polar cap more than 50% of the D_p field is due to the longer period component, which is identical with an enhanced $S_q{}^p$ field.

(v) The strength of electric field to produce SP-and AEJ-components of the present example of a sharp negative bay field will be estimated from the observed current intensities. The ionospheric conductivity under calm condition has been estimated by MATUURA (1961), based on the standard model atmosphere and temperature profile. The evaluated magnitudes of Pederson and Hall conductivities are 5.2 and 19 MKS respectively. Then, the electric field to produce the Hall current of about 140 amp/km of the SP-component in the polar cap area must be about 7 volts/km, which can be produced by lateral slipping of about 1.4 km/sec in velocity between the lines of geomagnetic force frozen in the lower border of magnetospheric plasma in the lower ionosphere and those of the non-ionized lower atmosphere (NAGATA and KOKUBUN 1962). If we assume that the lines of geomagnetic force are approximately electric equipotential lines, then the electric field near the magnetopause of 10 earth's radii in geocentric distance is about 0.23 volts/km, and the velocity of circulative motion of the magnetospheric low energy plasma there is estimated at about 5.8 km/sec.

As NAGATA and KOKUBUN (1962) pointed out for the case of the $S_q{}^p$ field, the SP field as a component of the D_p field could be produced by an enhanced circulation of the magnetospheric low energy plasma driven by an enhanced solar wind of more than 500 km/sec in velocity.

The electric field responsible for the auroral electrojet must be of a different mechanism from that of the *SP* electric field, because the activated area of the auroral electrojets is confined to the area of a narrow stripe in shape. In the present example of a sharp negative bay, the ratio of the length in geomagnetically E-W direction to the width in N-S direction of the activated narrow area amounts to as large as about 25. Let us now consider electric currents produced in high conductive auroral zones having such a form by electric field $\boldsymbol{E}^{\circ}=(E^{\circ}{}_{L}, E^{\circ}{}_{T})$, where E_L and E_T denote respectively the electric field components along the auroral zone and perpendicular to it. Assuming that number densities of electrons and ions increase abruptly by impinging of auroral electron beam in the auroral zone activated area, Hall conductivity σ_H and Pederson conductivity σ_p will increase to σ'_H and σ'_p respectively. Then, electric current $J_L(AEJ)$ along the auroral zone will be expressed as

$$J_L(AEJ)=\sigma_H\frac{k_H}{k_p}E^{\circ}{}_{T}+\frac{\sigma^2{}_pK_p{}^2+\sigma^2{}_HK_H(K_H-1)}{\sigma_pK_p}E^{\circ}{}_{L}, \qquad (2\text{–}1)$$

where

$$K_H=\sigma'_H/\sigma_H, \quad k_p=\sigma'_p/\sigma_p. \qquad (2\text{–}2)$$

It has been deduced in the previous discussion on the origin of the *SP* fleld that the *SP* electric field which is almost perpendicular to the auroral zone will be about 7 volts/km in intensity. This field must affect the auroral zone as a part of $E^{\circ}{}_{T}$. As will be seen in (2–1), the increased conductivity of the auroral zone does not intensify the electric current produced by the *SP* electric field, because k_H/k_p will be conserved approximately as unity regardless of enhancement of σ_H and σ_p in the auroral zone. Hence, to produce J (AEJ) another source of electric field $\boldsymbol{E}^{\circ}=(E^{\circ}{}_{L}, E^{\circ}{}_{T})$ has to be considered.

The magnitude of $J\,(AEJ)$ obtained from the present example is about 400 amp/km. If we assume that $k_p=k_H=10$, then either $E^{\circ}{}_{T}=21$ volts/km or $E^{\circ}{}_{L}=0.57$ volts/km can be responsible for the observed magnitude of $J\,(AEJ)$. When $k_p=k_H=10^2$, then $E^{\circ}{}_{T}=2.1$ volts/km or $E^{\circ}{}_{L}=0.057$ volts/km is required. These values of $E^{\circ}{}_{T}$ and $E^{\circ}{}_{L}$ in the lower ionosphere correspond to the electric field in the magnetosphere of 6.5 earth's radii in geocentric distance as given in Table II–3.

According to Nagata and Oguti (1961), the magnitude of k for moderate auroral zone disturbances is between 10 and 10^2. It may be presumed therefore that, in the case of a sharp negative bay, 1 volt/km or less in the transverse direction $(E^{\circ}{}_{L})$ or 0.05 volts/km or less in the longitudinal direction $(E^{\circ}{}_{L})$ will be created as an additional electric field around 6.5 earth's radii in geocentric dis-

Table II-3. Electric fields corresponding to the auroral electrojet.

a. Electric field responsible for SP-componenet ($T \geqq 6$ hours).

	Ionosphere	Magnetosphere
Electric field	7 volt/km	0.23 volt/km
Velocity	1.4 km/sec	5.8 km/sec

b. Electric field responsible for AEJ component ($T < 6$ hours).

	Ionosphere		Magnetosphere	
	Transverse (E°_T)	Longitudinal (E°_L)	Transverse (E°_T)	Longitudinal (E°_L)
$k_H = k_P = 10$	21 (volt/km)	0.57 (volt/km)	1.0 (volt/km)	0.046 (volt/km)
$k_H = k_P = 10^2$	2.1	0.057	0.1	0.005

tance near the equatorial plane in the magnetosphere. As seen in the table, the longitudinal electric field is much more effective than the transverse field.

(2) Broad large positive and large negative bays on Sept. 9, 13^h–18^h *UT*

Fig. 2–7 illustrates the horizontal component variation of the geomagnetic disturbances from 9^h to 18^h *UT* on September 9, 1958 observed at stations in the northern and southern polar regions. In the northern polar region, a large negative bay of 500–600γ in magnitude was observed at Point Barrow, College, Meanook and Fort Churchill which are located in the geomagnetic local morning area of the auroral zone, whereas a positive bay of 300–400γ in magnitude was observed at Reykjarvik and Kiruna which are located in the local afternoon area of the auroral zone.

In the southern polar region, a negative bay of 400γ was observed in Macquarie Island in the geomagnetic local morning area, while a positive bay of 150γ was observed at Mawson in the local afternoon area (Mawson is only 3 degrees higher in the corrected geomagnetic latitude than the maximal auroral zone stations such as Reykjavik or Kiruna). It will be concluded therefore that large negative and positive bays took place simultaneously in the both auroral zones, the former in the morning side and the latter in the afternoon side.

With regard to an approximately conjugate pair of Thule and Vostok, the horizontal component varied quite similarly to each other during the best-developed stage of the bay in the auroral zone between 13^h and 18^h *UT*. However, the conjugate relationship between the two stations was rather poor in the pre-bay and beginning stages.

A similar tendency is noticed also in an approximately conjugate pair of Murchison Bay and Mirny in the polar cap area. With regard to a conjugate pair of Cape Wellen and Macquarie Island near the auroral zone, the similarity of simultaneous *H*-variation was extremely good for the well-developed stage of 13^h–18^h *UT*, but the conjugate relationship was rather poor in the beginning stage.

The above-mentioned tendency that the conjugate relationship is extremely good for the well-developed stage but is rather poor for the beginning stage of bays has been well confirmed with regard to a number of bays observed in the conjugate pair of the Syowa Station and Reykjavik.

As shown in Fig. 2–7 (a)–(b), both negative and positive bays are approximately in their best-developed stage at 14^h 40^m and at 15^h 00^m *UT* in most sta-

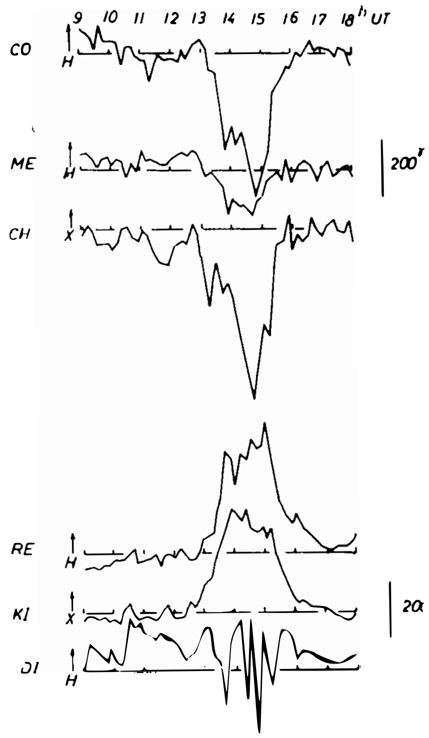

(a)

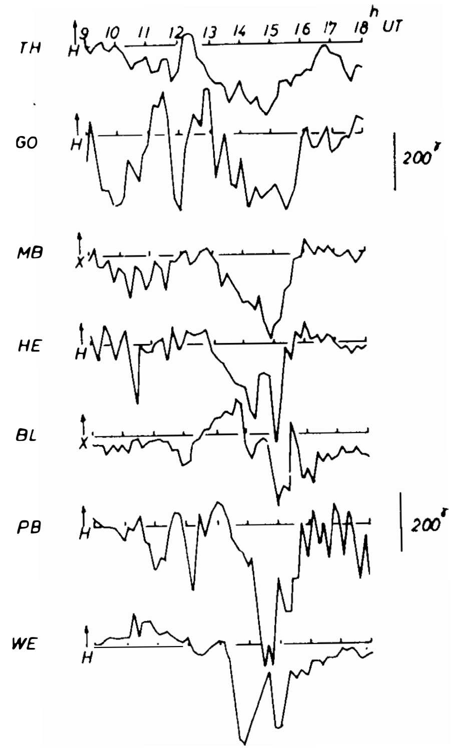

(b)

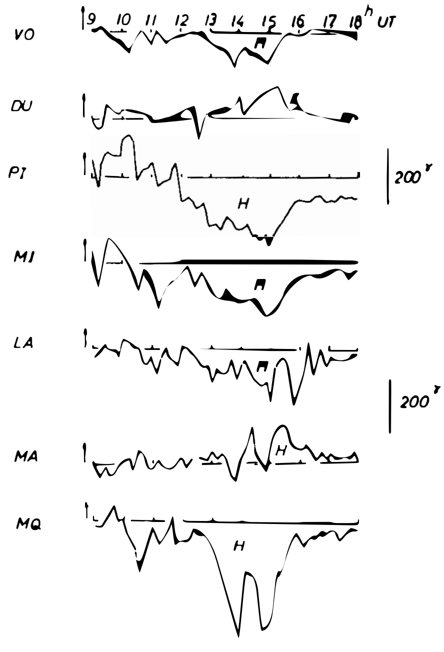

(c)

Fig. 2-7. Typical examples of geomagnetic bay (Sept. 9, 1958).

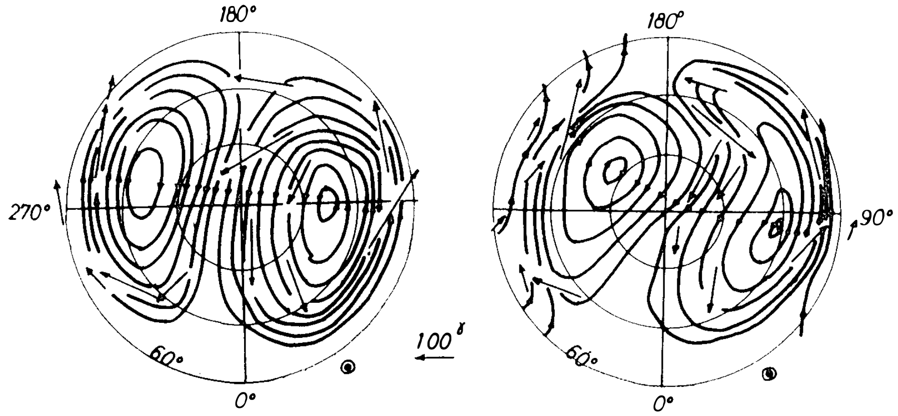

Fig. 2–8(a). Instantaneous D_P field at $14^h\ 40^m$, Sept. 9, 1958 in the northern polar region.
Left: $T_0 \geqq 6$ hours.
Right: $T_0 < 6$ hours.

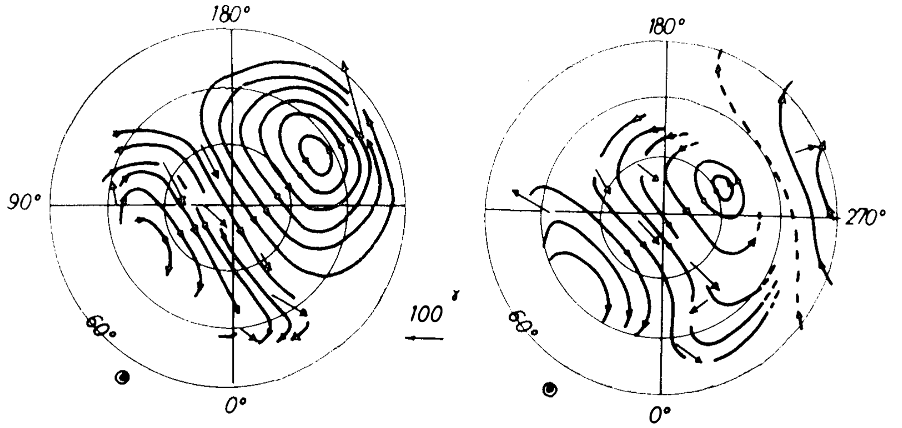

Fig. 2–8(b). Instantaneous D_P field at $14^h\ 40^m$, Sept. 9, 1958 in the southern polar region.
Left: $T_0 \geqq 6$ hours.
Right: $T_0 < 6$ hours.

tions, the equivalent ionospheric current systems for these two times have been constructed based on the data in Fig. 2–7. The obtained current patterns, for the longer period component (larger than 6 hours in period) and the shorter period component (shorter than 6 hours in period) and for the northern and southern regions, are separately illustrated in Fig. 2–8 (at the time of $14^h\ 40^m$ *UT*) and in Fig. 2–9 (at the time of $15^h\ 00^m$ *UT*).

The characteristic parameters obtained from these diagrams are summarized in Table II–4.

Comparing the current patterns of the present case where a broad negative bay on the early morning side and a positive bay on the evening side took place simultaneously (Figs. 2–8 and 2–9) with those of a case where a sharp negative bay

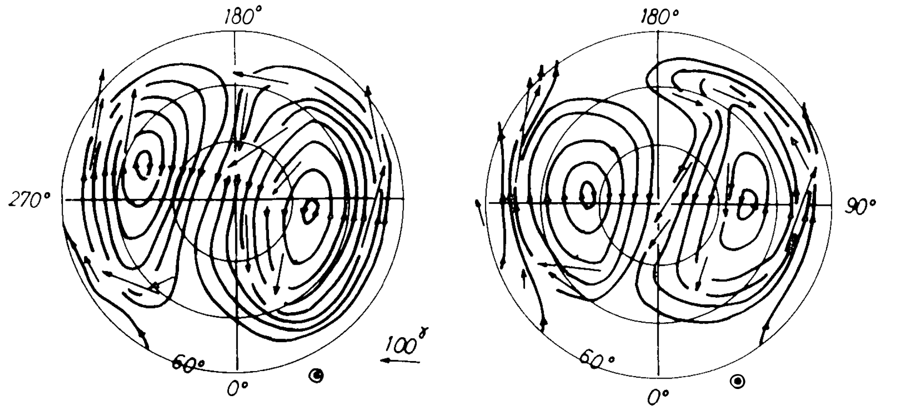

Fig. 2–9(a). Instantaneous D_p field at $15^h\ 00^m$, Sept. 9, 1958 in the northern polar region.
Left: $T_0 \geqq 6$ hours.
Right: $T_0 < 6$ hours.

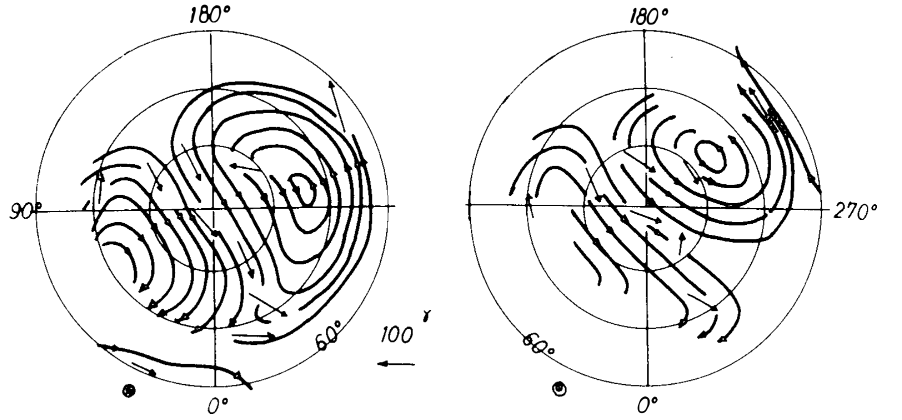

Fig. 2–9(b). Instantaneous D_p field at $15^h\ 00^m$, Sept. 9, 1958 in the southern polar region.
Left: $T_0 \geqq 6$ hours.
Right: $T_0 < 6$ hours.

was absolutely dominant (Figs. 2–5 and 2–6), and comparing the northern patterns with the corresponding southern patterns, the longer period component patterns with the shorter period component ones, and also the polar cap current density with the auroral zone one, the following characteristics may be pointed out.

(i) In the present case, a broad negative bay and a positive bay took place simultaneously on the early morning side and the dusk side respectively in the polar regions. The total currents of the positive bay is a little larger than those of the broad negative bay. The current patterns and current intensities in the northern and southern polar regions are approximately symmetric with each other with respect to the geomagnetic coordinate.

(ii) The current systems of the longer period component in both polar re-

Table II-4. Characteristic parameters of D_p field of bays on Sept. 9.

a. Long period component at 14^h 20^m in UT (See Fig. 2-8).

	Northern polar region	Southern polar region
Direction	9^h	8^h
Current vorticies	$73°$, 3^h	$74°$, 2^h
	$74°$, 16^h	$75°$, 13^h
Intensity		
polar cap	177 amp/km	125 amp/km
auroral zone (a.m.)	208 amp/km	208 amp/km
auroral zone (p.m.)	229 amp/km	—

b. Short period component (To <6 hours) at 14^h 40^m (See Fig. 2-8).

	Northern polar region	Southern polar region
Direction	6^h	7.5^h
Intensity		
polar cap	146 amp/km ($\Phi_m=67°$)	135 amp/km
eastward *AEJ*	187 amp/km ($\Phi_m=65°$)	
westward *AEJ*	229 amp/km ($\Phi_m=67°$)	208 amp/km ($\Phi_m=-68°$)

c. Long period component (To ≧6 hours) at 15^h 00^m (See Fig. 2-9).

	Northern polar region	Southern polar region
Direction	10^h	9^h
Current vorticies	$73°$, 3^h	$75°$, 3^h
	$75°$, 16^h	$73°$, 15^h
Intensity		
polar cap	177 amp/km	125 amp/km
auroral zone (a.m.)	208 amp/km	156 amp/km
auroral zone (p.m.)	229 amp/km	—

d. Short period component (To <6 hours) at 15^h 00^m (See Fig. 2-9).

	Northern polar region	Southern polar region
Direction	9^h	7^h
Intensity		
polar cap	125 amp/km	104 amp/km
westward *AEJ*	302 amp/km ($\Phi_m=65°$)	187 amp/km ($\Phi_m=-61°$)
eastward *AEJ*	239 amp/km ($\Phi_m=65$)	—

gions are quite similar to those of the S_q^p field. The ratio of the current density in the auroral zone to that in the center of polar cap is 1.1–1.3 in the north polar region and 1.2–1.4 in the south polar region. This indicates that there is no particular auroral zone enhancement in this component. The geometry of current pattern in the south is not exactly the same as that in the north; differences between the south and the north in the direction of polar cap current and the location of centers of current vortices amount to 1 hour in local geomagnetic time and 1–2 degree in geomagnetic latitude.

(iii) In the short period component patterns, intense westward and eastward auroral electorojets are dominant in the both auroral zones. The ratio of intensity of westward *AEJ* to the polar cap current density is 1.7–2.5 in the north and 1.6–2.3 in the south. In regard to the eastward *AEJ*, the ratio amounts to 1.5–2.0 in the north. (The ratio cannot be determined in the south because of lack of auroral zone stations on the afternoon side.) It will be concluded, therefore, that the eastward *AEJ* and westward *AEJ* are nearly equal in intensity, and the average *AEJ* intensity is about twice as large as the polar cap current density. The average *AEJ* intensity in the present case having twin vortices is definitely smaller than the *AEJ* intensity of a sharp negative bay in which only a current vortex is dominant. The general feature of current patterns of the shorter period component for the present case of twin current vortices is closely similar to that of the typical *DS* field proposed by NAGATA (1952), NAGATA and KOKUBUN (1962) and NAGATA and IIJIMA (1964).

(iv) In the present case, about 50% of the disturbances in the polar cap area is due to the *SP* field, whereas less than 40% of the disturbances in the auroral zone is due to the *SP* field, the remaining more than 60% being attributed to the auroral electrojet.

(v) Electric field corresponding to the present bay can also be estimated based on MATUURA's evaluation (1961) of the ionospheric conductivity.

For the *SP* field in the polar cap area, the estimated electric field amounts to 9 volts/km in the lower ionosphere. Transferring this electric field to the magnetosphere at 10 earth's radii in geocentric distance, the electric field there be-

Table II-5. Electric field corresponding auroral electrojet.

a. Electric field for SP-component.

	Ionosphere	Magnetosphere
Electric field	9 volt/km	0.3 volt/km
Velocity	1.8 km/sec	7.5 km/sec

b. Electric field for AEJ component.

	Ionosphere transverse (volt/km)	Ionosphere longitudinal (volt/km)	Magnetosphere transverse (volt/km)	Magnetosphere longitudinal (volt/km)
$k_H = k_p = 10$	17	0.43	0.91	0.035
$k_H = k_p = 10^2$	1.7	0.004	0.09	0.0003

comes 0.3 volts/km, which can be produced by a circulation of low-energy magnetospheric plasma of 7.5 km/sec in velocity.

As for *AEJ* field, an additional electric field $E^{\circ}{}_T = 17$ volts/km or $E^{\circ}{}_L = 0.43$ volts/km is necessary in the auroral zone ionosphere for $k_H = k_p = 10$.

The required value of $E^{\circ}{}_T$ or $E^{\circ}{}_L$ in the case of $k_H = k_p = 10^2$, and the corresponding electric fields in the magnetospheric level of 6.5 earth's radii in geocentric distance are summarized in Table II–5.

In summarizing the present studies of the conjugate relationship for individual geomagnetic bays, the following facts may be pointed out as the major characteristics.

(a) The geomagnetic conjugate relationship holds well for the best-develped stage of geomagnetic bays, but the conjugacy is definitely poorer in the beginning stage.

(b) The distribution pattern of the longer period component (longer than 6 hours in duration) of polar disturbance sequence including a bay or bays can be interpreted as an enhanced pattern of the $S_q{}^p$ field which has no particualr auroral zone augmentation. For this component (*SP* field), the geomagnetic conjugate relationship holds satisfactorily well. The *SP* field may be ascribed to an increase of circulation velocity of magnetospheric low energy plasma near the magnetopause from about 3 km/sec under calm condition for the $S_q{}^p$ field to 5–10 km/sec under moderately disturbed condition of the *SP* field.

(c) The distribution pattern of the shorter period componet (shorter than 6 hours in duration, consisting mostly of a bay or bays) can be attributed to auroral electrojet (s) and its (or their) countercurrent in the ionosphere. The conjugacy for this *AEJ* (auroral electrojet) component is a little poorer than that for the *SP*-component with regard to intensity. However, a sharp negative bay in the south corresponds to a sharp negative bay in the north, and a broad negative bay and a co-existing broad positive bay in the south correspond to the same configuration in the north. The *AEJ* field may be ascribed to creation of an additional longitudinal electric field of 5–50 mV/km (or to an additional transverse electric fleld of 0.1–1 V/km) in the magnetospheric plasma space which is connected to the earth's auroral zones by the lines of geomagnetic force.

CHAPTER III. CONJUGATE RELATIONSHIP OF STORM SUDDEN COMMENCEMENTS (SSC) BETWEEN SYOWA STATION AND REYKJAVIK

III-1. Introduction

The storm sudden commencement (*SSC*) may be defined as a sudden change of the geomagnetic field with duration of 1–6 minutes at the beginning of a magnetic storm.

In regard to the structure of the *SSC* field, OBAYASHI and JACOBS (1957) have proposed to divide it into two parts, namely, a world-wide component approximately symmetric around the geomagnetic axis, which is called D_{st} (*SSC*), and an additional part of disturbances confined mostly to the polar region, which is called *DS* (*SSC*). A number of different theories have been proposed for interpretation of the *SSC* field. It seems that many workers have agreed in ascribing D_{st} (*SSC*) to a transient phenomenon of a compression of the geomagnetic cavity by the front of an intensified storm solar wind. With regard to the origin of *DS* (*SSC*), at least two different concepts of theoretical interpretaion have been proposed, *i. e.* a dynamo theory (NAGATA and ABE, 1955; OBAYASHI and JACOBS, 1957; OGUTI, 1957) and a hydromagnetic theory (PIDDINGTON, 1960, 1962; WILSON and SUGIURA, 1961; NAGATA and KOKUBUN, 1962; VESTINE and KERN, 1962). The chief purpose of the present work on the *SSC* problems is a detailed examination of the conjugate relationship for the polar *SSC* field, using the simultaneous data obtained at the conjugate stations, Syowa Station and Reykjavik, during the period from 1959 to 1961, and critical discussion of the analyzed result based on the existing theories.

III-2. Similarity and simultaneity of *SSC*s between the conjugate points

Simultaneous data of 66 *SSC*s observed at Syowa Station and Reykjavik during three years of 1959–1961 were picked up as materials for the present study. Two examples of these data are illustrated in Fig. 3–1. All these *SSC*s occurred almost simultaneously at the conjugate stations and their *H*-component traces are similar to, and in-phase with, each other, whereas their *D*-component traces are anti-phase with each other.

Based on the IGY data obtained in the USA region, MATSUSHITA (1962) proposed to classify *SSC*s into the following three different types:

(1) *SSC*: this type is characterized by an ordinary sudden increase of *H*-component.

(2) ^{-}SSC: this type is the same as what has been called *SSC** (NAGATA and ABE, 1955) and is characterized by a sudden decrease preceding the main positive increase of *H*-component.

(3) SSC^{-}: this type first shows an ordinary field increase which is followed by a field decrease to the lower level than the initial pre-*SSC* level; the reversed *SSC* is also included in this type.

Adopting MATSUSHITA's classification in the present analysis, the occurrence tendency of *SSC*s at the conjugate stations has been obtained as given in Table III-1.

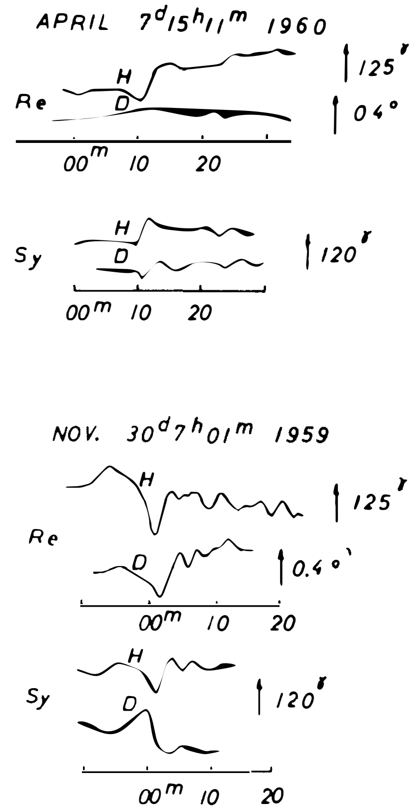

Fig. 3-1. Examples of SSCs observed simultaneously at Syowa Station (Sy) and Reykjavik (Re).

Table III-1. Statistical summary of occurrence of three different types of SSC at Syowa Station and Reykjavik.

Total number	Morning side (23^h–11^h)		Afternoon side (11^h–23^h)	
	34		32	
	Reykjavik	Syowa Station	Reykjavik	Syowa Station
SSC	8	8	6	4
^{-}SSC	13	13	19	20
SSC^{-}	13	13	7	8
With *PRI*	13	13	19	20
Without *PRI*	21	21	13	12

Remark: *PRI* denotes the preliminary reverse impulse of ^{-}SSC.

On the morning side (23^h–10^h in local geomagnetic time) all *SSC*s at the Syowa Station are of the same type as those observed simultaneously at Reykjavik without exception. On the afternoon side, 90% of the total *SSC*s are of

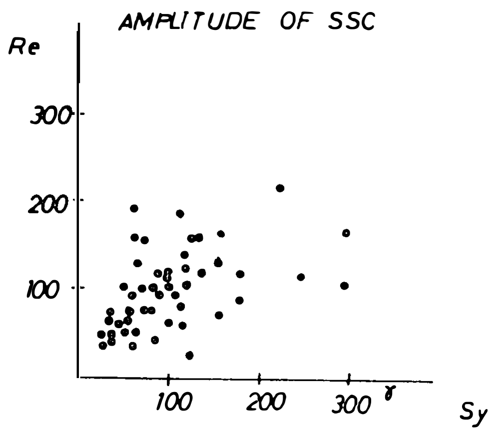

Fig. 3–2. Correlation diagram of amplitude of SSCs between Syowa Station (Sy) and Reykjavik (Re).

the same type at the conjugate points.

The general tendency of statistical distribution of three different types of *SSC*s dependent on local time at Syowa Station and Reykjavik is in good agreement with that for the auroral zone stations such as Point Barrow and College in MATSUSHITA's result (1962).

The occurrence frequency of *SSC*s with *PRI* is almost the same at the conjugate stations; 38% of the morning *SSC*s are preceded by *PRI*, whereas 62% of the afternoon *SSC*s are associated with *PRI*. This statistical result supports previous statistical results obtained by NAGATA and ABE (1955) and MATSUSHITA (1962).

The correlation of amplitude of *SSC*s between Syowa Station and Reykjavik is illustrated in Fig. 3–2. In this diagram, the amplitude of three types of *SSC* is defiend as follows: The amplitude of (ordinary) *SSC* is the change of horizontal force from the pre-*SSC* value to the peak of positive impulse; that of ^{-}SSC is defined as the difference of horizontal force from the bottom of *PRI* to the peak of main positive impulse; that of SSC^{-} is defined as the difference between the peak of positive impulse and the bottom of subsequent reverse impulse.

The correlation coefficients of thus defined amplitudes between the conjugate points amount to 0.69. It may be concluded from the result that the amplitudes of *SSC*'s at the conjugate points are fairly well correlated with each other, cases where the amplitudes at the two points are nearly identical being dominant so far as they are less than 200γ.

III–3. Polarization of *SSC*s at the conjugate points

It was found by WILSON and SUGIURA (1961) that the polarization vector of *SSC* in high latitudes makes an elliptic counterclockwise rotation on the morning side (22^h–10^h in geomagnetic local time) and an elliptic clockwise rotation on the afternoon side when viewed downward along the lines of geomagnetic force. Based on the magnetograms at College in Alaska and Macquarie Island, they suggested further that the conjugate relationship might hold for the polarization characteristics of *SSC*. This view of WILSON and SUGIURA was opposed by MATSUSHITA (1962) who analyzed the IGY *SSC* events observed mostly in the USA region.

In the present work, the polarization characteristics of *SSC*s will be examined in some detail using the exactly simultaneous records obtained at Syowa Station and Reykjavik in order to review the above-mentioned discrepancy between

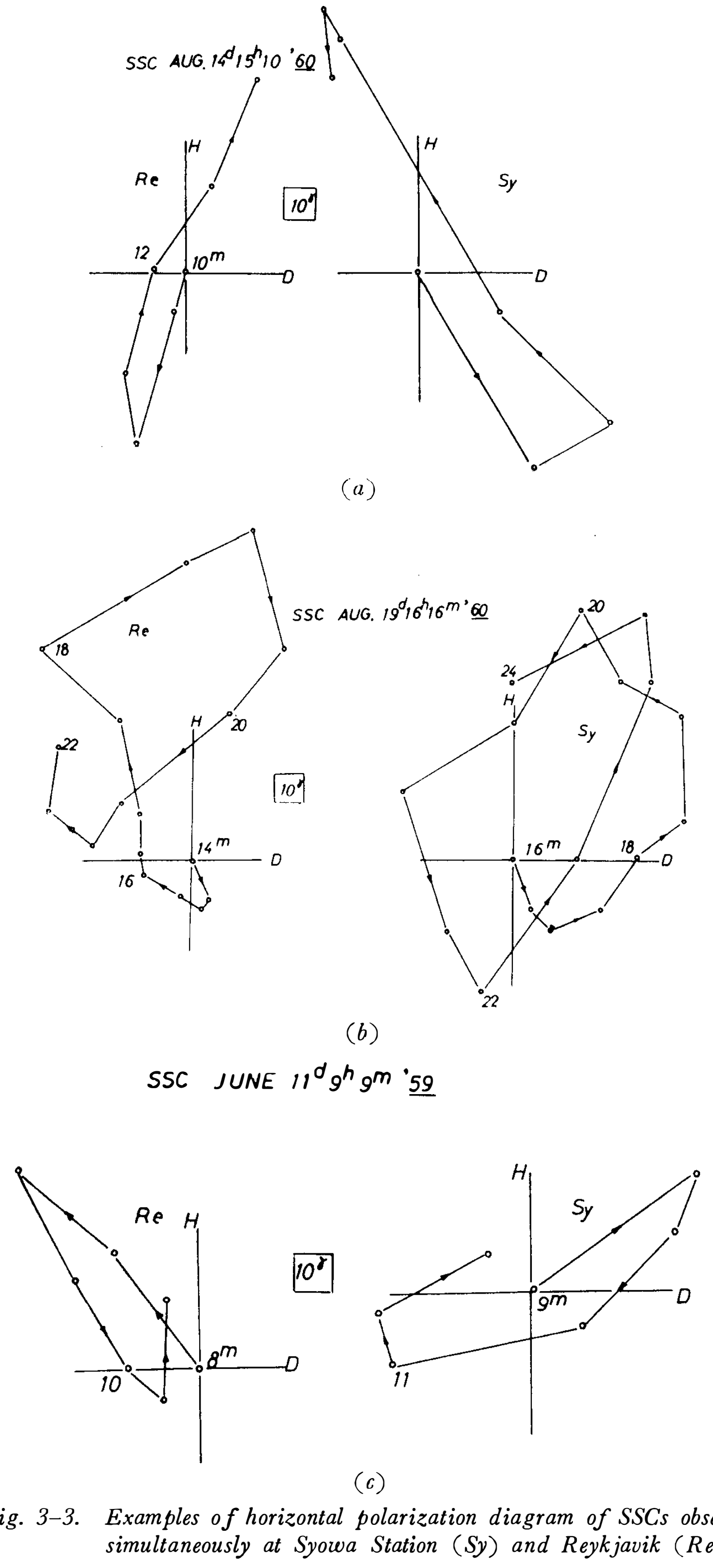

Fig. 3-3. Examples of horizontal polarization diagram of SSCs observed simultaneously at Syowa Station (Sy) and Reykjavik (Re).

MATSUSHITA and WILSON-SUGIURA with the aid of possible conjugate relationships of the pheomena concerned.

The polarization characteristics of the 66 typical examples of *SSC*s which were dealt with in the preceding section were examined individually. Three examples of the simultaneous polarization diagrams of *SSC*s at Reykjavik and Syowa Station are illustrated in Fig. 3-3.

(a) ^{-}SSC on August 14, 15^{h} 10^{m}, 1960

This is an example of ^{-}SSC on the afternoon side, showing a clockwise rotation at Reykjavik and a counterclockwise rotation at Syowa Station. The major axis of the elliptic polarization is deviated from the geomagnetic north toward east by 25° at Reykjavik and by −25° at Syowa Station. The absolute magnitudes of this *SSC* are approximately the same at the conjugate stations.

(b) ^{-}SSC on August 19, 16^{h} 16^{m}, 1960

This is an example of a little complicated ^{-}SSC in the afternoon. The conjugacy of polarization is satisfactorily well.

(c) SSC^{-} on June 11, 09^{h} 09^{m}, 1959

This is an example of SSC^{-} on the morning side. The rotation of polarization is counterclockwise at Reykjavik and clockwise at the Syowa Station.

The polarization characteristics of the 66 *SSC*s thus examined are summarized in Table III-2.

Table III-2. Polarization characteristics of SSCs at the conjugate stations.

	Morning side (23^{h}–11^{h})		Afternoon side (11^{h}–23^{h})	
Total number of *SSC*	34		32	
Polarization	Reykjavik	Syowa Station	Reykjavik	Syowa Station
Clockwise	3	24	17	5
Counterclockwise	23	2	9	20
Undeterminable	8	8	6	7

On the morning side, 88% of *SSC*s whose polarization characteristics can be determined have the counterclockwise rotation at Reykjavik while 92% of corresponding *SSC*s at Syowa Station are of the clockwise rotation. On the afternoon side, this tendency is just reversed; 65% of *SSC*s at Reykjavik are clockwise and 80% of *SSC*s at Syowa Station are counterclockwise.

This result indicates that the polarization characteristics at the conjugate stations are identical with respect to the direction of the line of geomagnetic force; namely, a counterclockwise rotation on the morning side and a clockwise rotation on the afternoon side as viewed along the direction of line of geomagnetic force. This general feature of rotation characteristics of the polarization of *SSC*s is in exact agreement with that pc-5 magnetic pulsations, which will be described in Chapter V. It will be concluded therefore that the present result on the

*SSC*s in the auroral zones seems to support WILSON–SUGIURA's view on the local time dependence of the polarization characteristics of polar *SSC*s and further verifies satisfactorily their suggestion of the geomagnetic conjugacy of polar *SSC*s.

III–4. Amplitude of *SSC* at the conjugate points

The local time dependency of amplitude of *SSC*s at Syowa Station and Reykjavik is illustrated in Fig. 3–4. This statistical result was obtained from the data of 90 *SSC*s in the years of 1959–1961, including the simultaneous 66 examples dealt with in the preceding sections.

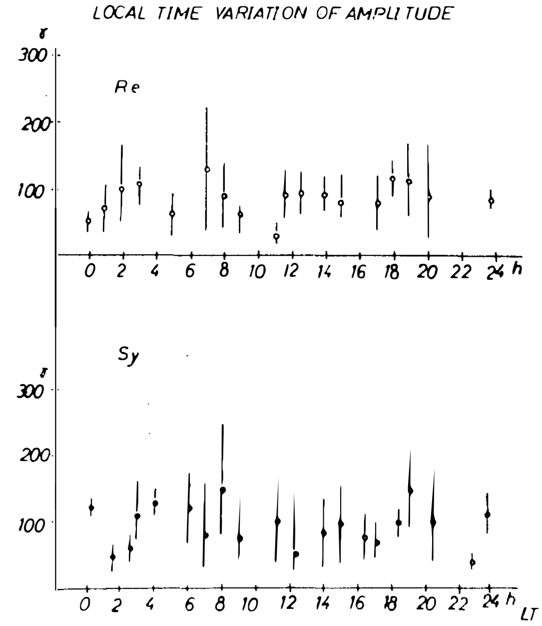

Fig. 3–4. Amplitude of SSCs vz local time.

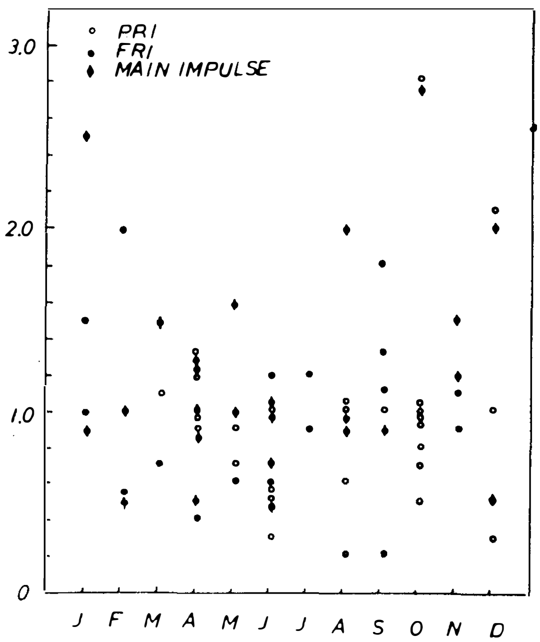

Fig. 3–5. Dependency of the ratio of SSC amplitude at Reykjavik to that at Syowa Station dependent on season.

No definite dependency of amplitude of *SSC* upon local time can be seen in this figure. This is a marked contrast to pc-5 magnetic pulsation, of which amplitude in the local morning is larger than that in the afternoon (See Chapter V). It will be noticed in Fig. 3–4, however, that the daily variations of the average amplitude of *SSC*s at the conjugate stations resemble each other in fair detail.

The seasonal dependency of the relative amplitude of *SSC*s between the Syowa Station and Reykjavik, *i. e.* the ratio $\Delta H_{Re}/\Delta H_{Sy}$, was examined with regard to magnitudes of the main positive impulse, the preliminary reverse impulse of ^{-}SSC and the subsequent reverse impulse of SSC^{-}, with the result as shown in Fig. 3–5. It seems likely in this diagram that the $\Delta H_{Re}/\Delta H_{Sy}$ ratio tends to become a little larger in the northern winter, but the scattering of plots is so remarkable that no definite dependency of the ratio on season can be confirmed.

III–5. *SSC*-oscillation at the conjugate points

According to Wilson and Sugiura (1961), more than 50% of *SSC*s observed in the north polar region are associated with pulsations of 2.5–10 minutes in period and 10–60 minutes in duration. They also reported that *SSC* oscillations of this kind are found at both College and Macquarie Island, an approximate conjugate pair.

In the present study, the *SSC*-oscillations will be examined in some details using the simultaneous rapid-run records at the conjugate points, Syowa Station and Reykjavik. Two typical examples of simultaneous *SSC*-oscillations observed at the conjugate stations are selected and subjected to the Fourier analysis to get their power spectra with respect to period. Main characteristics of the power spectra of these *SSC*-oscillations, illustrated in Fig. 3–6 (a) and (b), will be summarized as follows:

(a) *SSC*-oscillation on August 19, 16^h 16^m, 1960

The power spectra at Syowa Station and Reykjavik are approximately the same. Maximum peak of the spectrum is 120 sec. at Reykjavik and 144 sec. at the Syowa Station.

(b) *SSC*-oscillation on December 7, 18^h 04^m, 1960

The spectra at Syowa Station and Reykjavik are quite similar to each other, the dominant period being 180 sec. at both stations.

It may be deduced from these results that *SSC*-oscillations at the conjugate

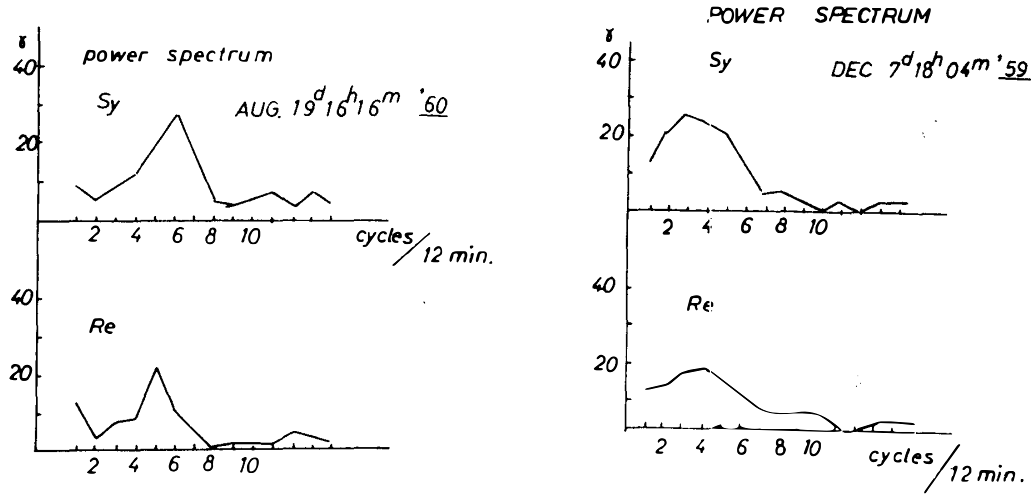

(*a*) (*b*)

Fig. 3–6. Frequency spectra of pulsation following SSC observed simultaneously at Syowa Station (Sy) and Reykjavik (Re).

points have the same power spectrum characteristics, their dominant period being 2–3 minutes, much shorter than that of pc-5 pulsations observed at the same conjugate points (See Capter V).

III-6. Rise time of *SSC* at the conjugate points

The rise time of *SSC*s observed at the conjugate stations will be compared as a representative parameter of *SSC* characteristics. It does not seem that the rise time of *SSC* has been definitely defined for ^{-}SSC and SSC^{-}. In the present comparison, the rise time (*Tr*) of ^{-}SSC, SSC^{-} and *SSC* will be temporarily defined in the following way:

Tr of *SSC*: time interval from the commencement to the maximum stage of main impulse. (Same as the widely adopted definition.)

Tr of ^{-}SSC: time interval from the commencement of preliminary reverse impulse to the maximum stage of main impulse.

Tr of SSC^{-}: time interval from the commencement of *SSC* to the bottom stage of subsequent reverse impulse.

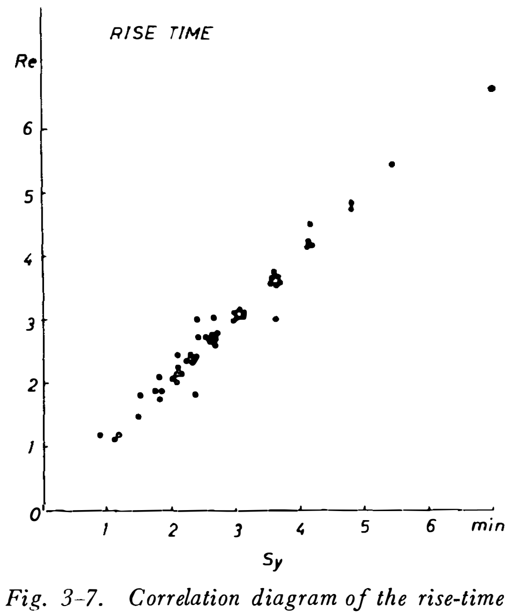

Fig. 3-7. Correlation diagram of the rise-time of SSC observed simultaneously at Syowa Station (Sy) and Reykjavik (Re).

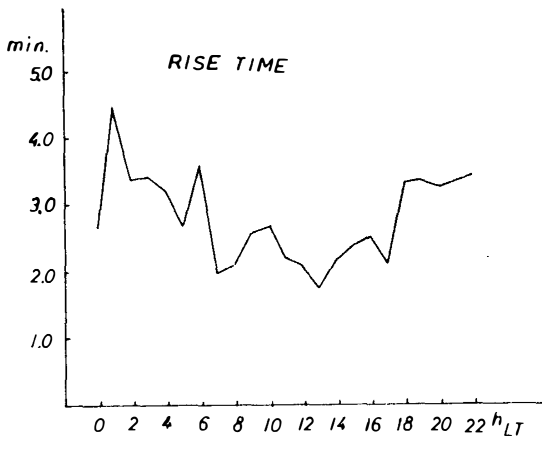

Fig. 3-8 Dependency of the rise-time of SSCs on local time.

The correlation of the rise time of *SSC*s thus defined between the Syowa Station and Reykjavik is illustrated in Fig. 3-7, which indicates that the rise time is always identical at the cojugate points. The observed rise time ranges between 1 min. and 7 min.

The local time dependency of the rise time also is examined, the statistical result being given in Fig. 3-8. It seems that the rise time is subject to a daily variation, the daytime rise time being shorter than the night-time one. The average rise time for 07^h–17^h in geomagnetic local time is 2.0–2.8 min. whereas that for 17^h–07^h amounts to 2.8–4.5 min.

III–7. Concluding remarks

Summarizing all conjugacy characteristics of storm sudden commencements observed simultaneously at Syowa Station and Reykjavik, the following conclusions will be drawn.

(1 *SSC*, ^{-}SSC and SSC^{-} occur almost simultaneously and their types are the same at conjugate points in the northern and southern auroral zones.

(2 The occurrence of preliminary reverse impulse is much more frequent on the afternoon side than on the morning side at both conjugate points.

(3 The polarization of disturbance vector in the horizontal plane is elliptic and is symmetric at conjugate points with respect to the geomagnetic coordinates. On the morning side (23^h–11^h) more than 88% of *SSC*s are of counterclockwise rotation and 73% of the afternoon *SSC*s are of clockwise rotation as viewed along the direction of the line of geomagnetic force.

(4 The transition of polarization between clockwise and counterclockwise rotations takes place at about the 11^h–23^h meridian in local geomagnetic time in both conjugate points in the auroral zones.

(5 The amplitude of *SSC*s seems to be only a little larger on the morning side than on the afternoon side, but the discrepancy is not remarkable.

(6 No definite seasonal variation is observed in the amplitude of *SSC*s in comparing the three phases of *SSC*s between conjugate points.

(7 *SSC*s at conjugate points have almost equal rise time. The average rise time in the daytime is 2.0–2.8 min. whereas that in the night-time 2.8–4.5 min.

Based on the observed facts summarized above, theoretical interpretations of physical mechanism of *SSC* phenomena will be critically reviewed.

As Jacobs and Obayashi (1957) showed, the main positive impulses of polar *SSC*s consist of D_{st} (*SSC*), which is represented by the eastward equivalent current around the geomagnetic axis, and *DS* (*SSC*) whose current pattern is almost equivalent to that of the $S_q{}^p$ field. It has been widely agreed that the D_{st} (*SSC*) field is caused by a sudden compression of the geomagnetic field confined to the magnetospheric space by a suddenly intensified storm solar plasma wind. This mechanism can certainly stand for the simultaneity and similarity of *SSC* observed at conjugate points, so far as the D_{st} (*SSC*) component is concerned.

As for the *DS* (*SSC*) field, Jacobs and Obayashi (1957) proposed a dynamo theory which maintain that a sudden increase in the polar cap ionization results in an additional *SD*-like current pattern through activation of the ionospheric dynamo in the polar cap area. As various kinds of observed evidence such as a sudden increase in cosmic noise absorption, X-ray burst, etc., occurring simultaneously with an *SSC* indicate that an *SSC* in associated with an abrupt increase in ionization in the polar cap ionosphere, and such an increase in ionization will take place simultaneously in both polar caps, JACOBS–OBAYASHI's theory seems to be qualitatively acceptable for interpretation of the *DS* (*SSC*) field. However, the amount of increase in ionization estimated from the directly observed evidence is too small when compared with the theoretically required amount, and the direction of ionospheric wind required for this dynamo theory of *DS* (*SSC*) is much deviated from that for the S°_{q} field.

PIDDINGTON (1960, 1962) and NAGATA and KOKUBUN (1962), on the other hand, have proposed hydromagnetic theories for the *SSC* phenomenon. According to NAGATA and KOKUBUN, the *DS* (*SSC*) field may be ascribed to a transient enhancement of the S_q^p field caused by a sudden additional twisting of the lines of geomagnetic force by the enhanced storm solar wind. This theory can stand well for the observed morphology of *DS* (*SSC*) field, because the *DS* (*SSC*) pattern is almost identical with the S_q^p one; moreover, this theory meets no difficulty with regard to the intensity of *SSC*, as obviously derived from the result of discussion of the D_p field (Chapter I). However, there is a morphological discrepancy between the S_q^p field and the polar *SSC* field, that is, the former shows marked seasonal variations of intensity, which is the strongest in regional summer and the weakest in winter, whereas no marked seasonal variations are observed in the latter. The seasonal variation of the S_q^p field is reasonably ascribed to the seasonal variation of electron and ion density in the polar ionosphere (NAGATA and KOKUBUN, 1962). If the *DS* (*SSC*) field is simply a transient state of static enhancement of the S_q^p field, a seasonal variation of amplitude of polar *SSC* would also be expected.

It will be considered, therefore, that the transference of *SSC* disturbance from the magnetosphere to the earth's surface through the ionosphere may not be due to such a quasi-stationary mechanism as considered for the S_q^p field but is probably due to propagation of hydromagnetic waves.

WILSON and SUGIURA (1961) have actually proposed a hydromagnetic wave theory for the *SSC* phenomenon. They found the polarization characteristics of *SSC* disturbances in the polar regions, such as described in Section III–3; they also reported that the polar *SSC* becomes ordinary *SSC* or ^{-}SSC depending on the initial direction of perturbation, whether it is northward or southward. As an example in Fig. 3–3(c) shows, SSC^{-} also can be ascribed to continuation of rotation of perturbation vector to a certain extent.

Since the polarization characteristics of *SSC* are essentially identical with those of pc–5 pulsations (See Chapter V), it would be natural, as WILSON and SUGIURA pointed out, to consider that *SSC* is attributed to a low frequency transverse hydromagnetic wave originating in the magnetosphere near the magnetopause. As the screening effect of the ionosphere for hydromagnetic waves of several minutes in period is not appreciable, there would be no considerable seasonal variation of amplitude of *SSC*s.

Then, it must be explained why the rotation of polarized perturbation vector is counterclockwise in the morning and clockwise in the afternoon viewed along the direction of the line of magnetic force and why ^{-}SSCs take place mostly on the afternoon side. WILSON and SUGIURA have suggested that the initial motion of the lines of force in the magnetosphere near the magnetopause, which is blown away from the sun by the intensified solar plasma wind, may result in the counterclockwise motion on the morning side and the clockwise one on the afternoon side. It seems likely that this intuitive interpretation is acceptable, although more precise mathematical analysis of the problem must be carried out based on appropriate initial and boundary conditions for the production and propagation of waves as well as for the non-uniformity of the magnetospheric plasma (KOKUBUN and NAGATA, 1965).

As for the preliminary reverse impulse (*PRI*) of ^{-}SSC, VESTINE and KERN (1962) suggested that possible charge separation of magnetospheric plasma in the sunward transition regions between the solar wind intersurface and the hydromagnetic shock front ahead of the stream intersurface, *i. e.* positive charge on the afternoon side and negative on the morning side, which may be caused by a sunward gradient of magnetic field produced by compressed magnetic field only within the transition region, can produce the equivalent ionospheric current pattern of *PRI*, as deduced by NAGATA (1952) and NAGATA and ABE (1955), provided that the separated electric charges are transferred along the lines of force to the polar ionosphere. In the term of production of hydromagetic waves in or near the sunward transition region in the magnetosphere, VESTINE-KERN's theory indicates that a magnetic field produced by the separated charges tends to distort the geomagnetic force outerward on the morning side and inward on the afternoon side near the inner boundary of the transition region. Then, this initial transverse distortion of the line of force projected on the earth's surface should be poleward on the morning side and equatorward on the afternoon side. Thus, it is possible that the local time dependency of ^{-}SSC is qualitatively interpreted by introducing a shock front within the magnetosphere produced by an impact on the magnetopause by an intense solar wind. Needless to say, a more precise mathematical examination of this problem is desired.

CHAPTER IV. CONJUGATE RELATIONSHIP OF SUDDEN IMPULSES (*SI*) BETWENEN SYOWA STATION AND REYKJAVIK

IV-1. Introduction

The sudden impulse (*SI*) of the geomagnetic field is defined as a sudden change of geomagnetic field of 1–6 minutes duration, which is observed world-widely and is not followed by a magnetic storm. The morphology of the *SI* phenemena observed in temparate and low latitude regions has been studied by

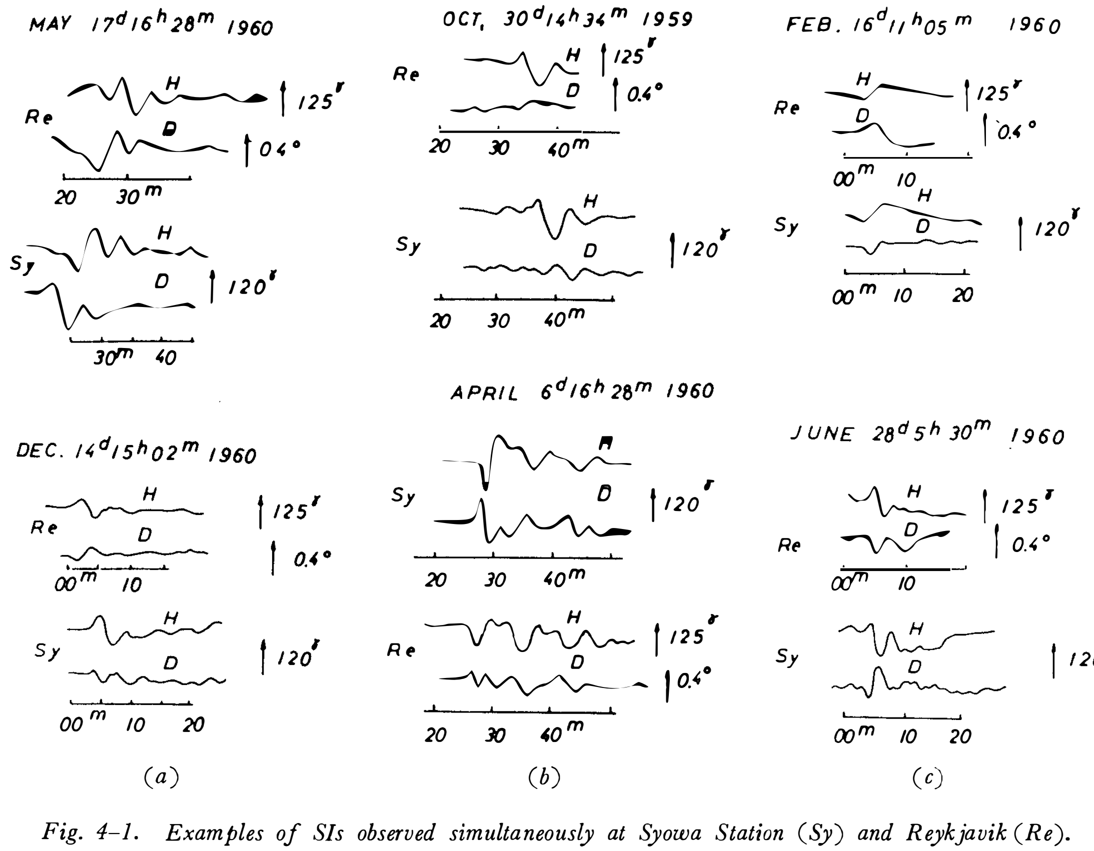

Fig. 4-1. Examples of SIs observed simultaneously at Syowa Station (Sy) and Reykjavik (Re).

MATSUSHITA (1962) and NISHIDA (1963).

In relation to the conjugate relationship of *SSC*, the *SI*s observed simultaneously at Syowa Station and Reykjavik will be examined in this chapter with special attention to their possible conjugate relationship. Six typical examples of *SI*s observed at the two stations are illustrated in Fig. 4–1. As shown in the figure, *SI*s are occasionally followed by pulsative disturbances, and some *SI*s are preceded by preliminary reverse impulses. MATSUSHITA (1962) proposed, therefore, to classify *SI* variations into several different types.

The definitions of *SI*, ^{-}SI and SI^{-} in MATSUSHITA's proposal are essentially the same as those of *SSC*, ^{-}SSC and SSC^{-} with respect to order of appearance of the preliminary reverse impulse or the subsequent reverse impulse with respect to the main positive impulse. In addition to these types of *SI*, MATSUSHITA has proposed the fourth type of *SI*, called $SI^{\ominus}$, which is defined as a sudden change with no positive impulse but definitely distinguishable from the reverse *SSC*.

In the present work, the local time dependence of occurrence of different types of *SI*s and their polarization characteristics at the conjugate stations will be chiefly dealt with.

IV–2. Simultaneity and similarity of *SI*s at the conjugate points

Simultaneous examples of 32 sudden impulses (*SI*) observed at Syowa Station and Reykjavik were picked up from the rapid-run magnetograms during the period of 1959–1960. As seen in Fig. 4–1, *H*-component traces of *SI*s observed at the conjugate stations are closely similar to each other, all phases being approximately in-phase, and their *D*-component traces are out-of-phase with each other. These characteristics of *SI*s are exactly the same as those of *SSC*s. Each of 32 examples of *SI*s is identified as one of the three types, *SI*, ^{-}SI or SI^{-}, no $SI^{\ominus}$ being found among these examples.

Types of the selected 32 examples are listed in Table IV–1 for the morning *SI*s and afternoon ones separately.

As shown in the table, an *SI* event is almost always of the same type at the

Table IV–1. Classification of SI types observed at the conjugate stations.

Type	Morning side 23^h–11^h		Afternoon side 11^h–23^h	
	Syowa Station	Reykjavik	Syowa Station	Reykjavik
SI	1	1	4	4
^{-}SI	5	5	8	7
SI^{-}	4	4	10	11
With *PRI*	5	5	8	7
Without *PRI*	5	5	14	15
Total	10		22	

conjugate points. This argument is proved right for individual 31 cases among the total 32 events. However, no definite dependency of occurrence of special type of *SI* on local time is found in the table.

IV-3. Polarization characteristics of *SI*s at the conjugate points

In regard to many aspects, the *SI* phenomenon resembles the *SSC* phenomenon. The polarization seems to be one of the common characteristics. Two examples of the polarization diagrams of *SI* as observed simultaneosly at Syowa Station and Reykjavik are illustrated in Fig. 4-2(a) and (b), and the polarization characteristics of 31 examples are summarized in Table IV-2.

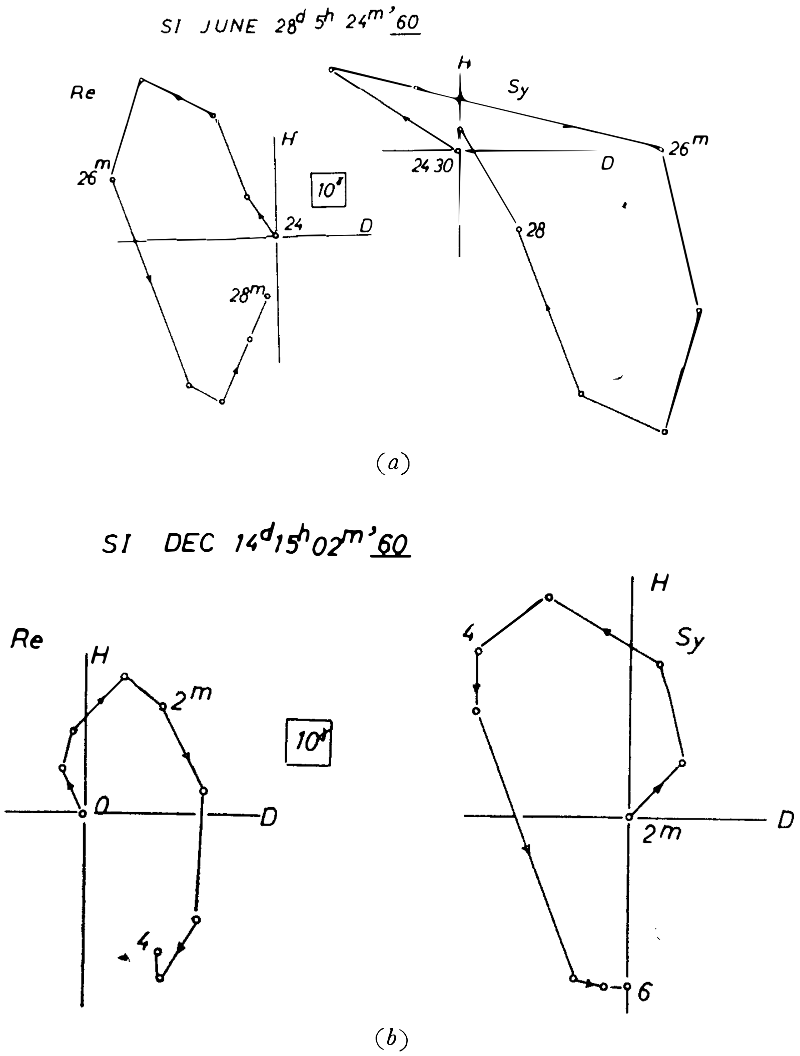

Fig. 4-2. Examples of horizontal poralization diagram observed simultaneously at Syowa Station (Sy) and Reykjavik (Re).

Table IV-2. Polarization characteristics of SIs observed at Syowa Station and Reykjavik.

Polarization rotation	Morning side (23^h–11^h)		Afternoon side (11^h–23^h)	
	Syowa Station	Reykjavik	Syowa Station	Reykjavik
Counterclockwise	1	8	13	3
Clockwise	8	1	3	13
Undeterminable	0	0	6	6
Total	9		22	

As is statistically obvious in the above table, the perturbation vector of *SI* rotates counterclockwise on the morning side and clockwise on the afternoon side as viewed along the direction of the line of geomagnetic force at the conjugate stations. This character is exactly the same as that of *SSC*.

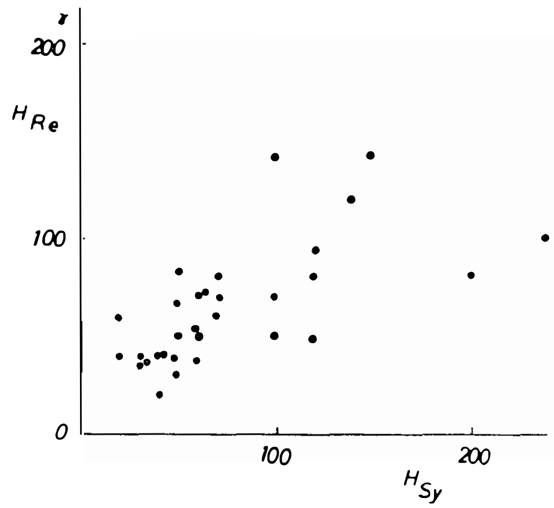

Fig. 4-3. Correlation diagram of amplitude of SIs observed simultaneously at Syowa Station (H_{Sy}) and Reykjavik (H_{Re}).

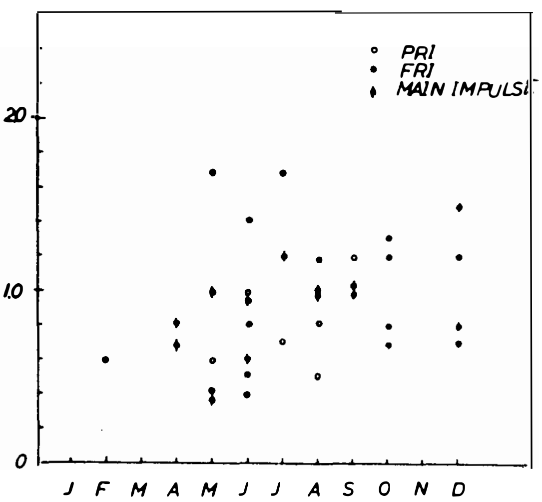

Fig. 4-4. The ratio of amplitude of SI at Reykjavik to that at Syowa Station versus season.

Amplitudes of *SI*s observed at Syowa Station are compared with those at Reykjavik in a correlation diagram in Fig. 4-3 where the amplitudes of ^{-}SI and SI^{-} are defined the same as for ^{-}SSC and SSC^{-}. The correlation coefficient amounts to 0.59, which is a little smaller than the correlation coefficient for *SSC*s at the same stations (See Chapter III).

The ratios $\Delta H_{Re}/\Delta H_{Sy}$ for the preliminary reverse impulse, for the main impulse and for the subsequent reverse impulse of *SI*s are plotted against season in Fig. 4-4 to examine possible seasonal variation of the ratio. As in the case of *SSC*s, no definite seasonal variation of $\Delta H_{Re}/\Delta H_{Sy}$ can be found in this diagram. This result may indicate that the *SI* phenomenon in the polar region is similar to the polar *SSC* phenomenon which cannot be simply attributed to fluctuations of the $S_q{}^p$ field.

IV-4. Concluding remarks

Characteristics of the *SI* phenomenon are common with those of the *SSC* phenomenon in many aspects. The common characteristics are:

(1) *SI*, ^-SI, and SI^- occur almost simultaneously with the same type at the conjugate points;

(2) The polarization characteristics are markedly dominant in *SI*s and are exactly the same as those of *SSC*s;

(3) No definite seasonal variation of amplitude of *SI*s can be detected.

The similarity between *SI*s and *SSC*s observed mostly in the temperate latitude region has already been pointed out by MATSUSHITA (1962) and NISHIDA (1963). In particular, NISHIDA has suggested that an *SI* is caused by an impulsive change of the magnetopause due to an impulsive change of the solar wind velocity or density. The conjugate relationship between the conjugate points in the auroral zone, summarized here for time of occurrence, types, amplitude and the polarization characteristics of *SI*s, seems to further support NISHIDA's mechanism of origin of *SI*s which is almost identical with the established mechanism of causation of *SSC*s. It may be worthwhile to note here, however, that the marked daily change in occurrence frequency of *PRI* is definitely recognized for *SSC*s but such a daily variation is not clear for *SI*s.

CHAPTER V.
CONJUGATE RELATIONSHIP OF PC–5 PULSATIONS BETWEEN SYOWA STATION AND REYKJAVIK

V–1. Introduction

Pc–5 magnetic pulsations with large amplitude (100–300γ in the auroral zone) and period of 100–500 sec. have been considered transverse hydromagnetic waves propagating from an outer part of the magnetosphere toward the polar ionosphere through the magnetospheric plasma. It has been already reported by NAGATA *et al.* (1963) that the pc–5 pulsations observed at conjugate points in the auroral zones are subject to the laws of conjugate relationship with regard to their time of occurrence, mode, amplitude and characteristics of polarization. The distribution of pc–5 pulsation in and near the northern auroral zone was examined in fair detail by WILSON (1963) and KOKUBUN and NAGATA (1965). According to them, amplitude of pc–5 pulsation is the largest in the auroral zone and decreases gradually toward the pole and decreases sharply toward the equator, the polarization characteristics remaininig invariant at least in the auroral zone and its equatorial side along the geomagnetic meridian: The frequency spectrum of pc-5 is of almost the same character having the same dominant period(s) in the auroral zone and in its equatorial side, suggesting that pc–5 pulsations are due to a hydromagnetic resonance in the magnetosphere. Based upon the existing knowledge mentioned above, pc–5 pulsations observed simultaneously at Syowa Station and Reykjavik will be examined in some details in the present work, their conjugate relationship for frequency spectra and mean amplitude being particularly dealt with as much as possible.

V–2. Similarity and simultaneity of pc–5 pulsations at the conjugate points

Fig. 5–1 shows three typical examples of pc–5 pulsations observed simultaneously at Syowa Station and Reykjavik. Examples (a) and (b) are morning pc–5 pulsations, taking place almost simultaneously at the two stations. The north components (H) of horizontal disturbances are parallel while the east components (D) are antiparallel at the conjugate stations. The dominant pe-

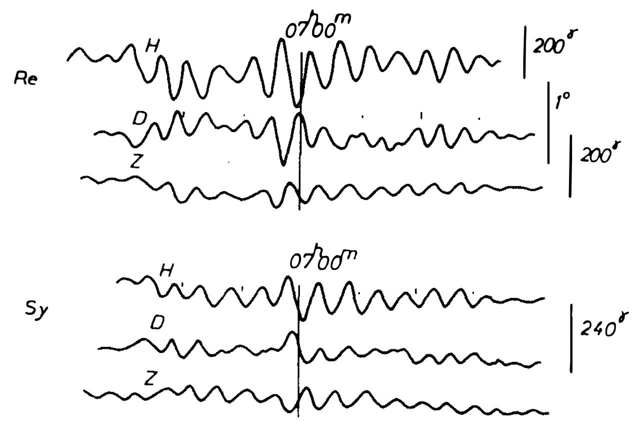

(*a*) *Sept. 18, 06h 30m–07h 30m, 1959.*

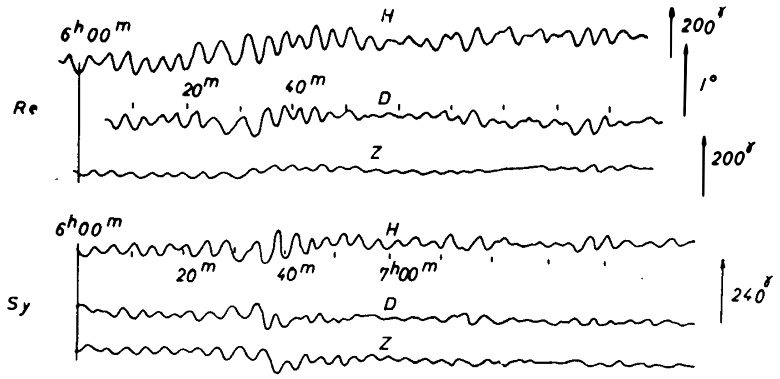

(*b*) *July 21, 06h 00m–07h 40m, 1959.*

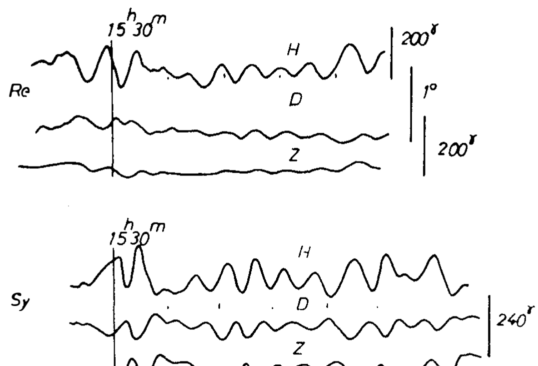

(*c*) *July 25, 15h 20m–16h 10m, 1959.*

Fig. 5-1. Example of pc–5 pulsations observed simultaneously at Syowa Station (Sy) and Reykjavik (Re).

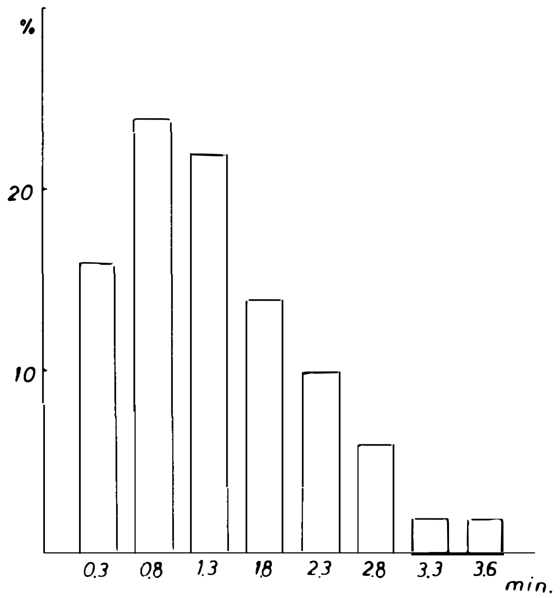

Fig. 5-2. Time-lag of same phase of pc-5 pulsations observed at Syowa Station and Reykjavik.

riod in the two pulsations are about 6 minutes at both stations. Example (c) is a case of afternoon pc–5 pulsation, whose dominant period being about 5.6 minutes at both stations. In this case also, the north components (H) are approximately parallel at the two stations.

Seventy-three examples of pc–5 pulsations are picked up from simultaneous rapidrun magnetograms obtained at Syowa Station and Reykjavik during two years, 1959–60. Generally speaking, the times of occurrence of these pulsations are almost simultaneous at the two stations and their wave forms are approximately parallel for the H-component and antiparallel for the D-component.

Assuming that the time-keeping for magnetograms at the two stations was sufficiently precise, it is noticed that all phases of pulsations at Reykjavik are always ahead those at Syowa Station by $0\sim2$ min., the average time lag being 1.2 min., as shown in Fig. 5–2.

The precision of time-keeping at Syowa Station was continuously checked by comparison with the standard time signals, so that a possible error in time should be smaller than 20 sec., which may be caused by a finite thickness of pen-records of Syowa Station magnetograms. The mean time lag (*i. e.* 1.2 min.) between geomagnetic events at Reykjavik and Syowa Station was kept almost constant for pc–5 pulsations, *SSC*s, *SI*s and also sharp commencements of negative bays, having no seasonal variation. We may temporarily conclude, therefore, that the time-lag is attributable to a possible relative error in time-keeping at these two stations.

Thus, we may conclude that pc–5 pulsations occur simultaneously at the conjugate stations. This conclusion is valid in any case, if errors of 1 min. in order of magnitude are allowable.

V–3. Polarization and amplitude of pc–5 pulsations at the conjugate points

Pc–5 pulsations are elliptically polarized in almost exactly the same way as *SSC*s. The rotations of perturbation vectors of pc–5 pulsations on the magnetic meridian plane as well as on a horizontal plane are illustrated in Fig. 5–3. In the figure, (a) and (b) are the examples of morning pc–5 pulsations. As seen in

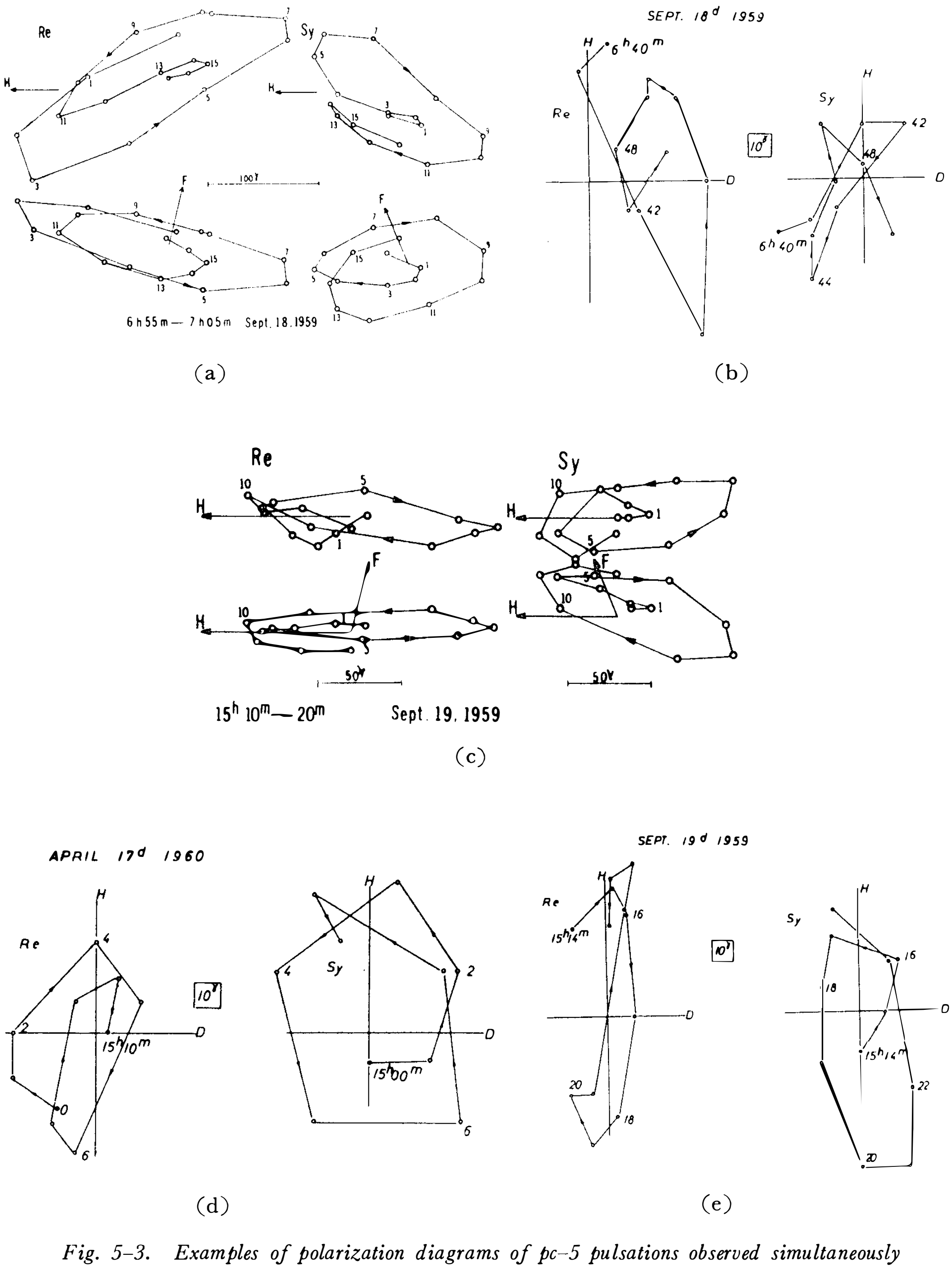

Fig. 5–3. Examples of polarization diagrams of pc–5 pulsations observed simultaneously at Syowa Station (Sy) and Reykjavik (Re).

the polarization diagrams, the major axis of polarization ellipse is approximately perpendicular to the direction of the line of geomagnetic force. This fact will indicate that pc–5 pulsations are dominantly transverse hydromagnetic waves. The rotation of horizontal vector $\boldsymbol{H}=(\Delta H, H\Delta D)$ is counterclockwise at Reykjavik and clockwise at Syowa Station, the polarization diagrams being symmetric with respect to the geomagnetic coordinates.

In the same figure, (c), (d) and (e) are the examples of afternoon pc–5 pulsations. These afternoon pc–5 pulsations also can be ascribed to transverse hydromagnetic waves. The rotation of elliptic polarization is clockwise at Reykjavik and counterclockwise at Syowa Station, being reverse to the case of moring pc–5 pulsations.

Among the selected 73 examples, 41 are morning pc–5 pulsations and the remaining 32 are afternoon ones. Polarization characteristics of all these examples are examined. Only for one example at Syowa Station and three examples at Reykjavik, the sense of rotation of polarization cannot be determined, because one of the two traces of the horizontal field variation ($\Delta \boldsymbol{H}$) is missing. So far as the magnetogram records are readable, the sense of rotation of polarization can be definitely determined. Statistics of the polarization characteristics of pc–5 pulsations thus obtained are summarized in Table V–1.

Table V–1. Polarization characteristics of pc–5 pulsations observed at Syowa Station and Reykjavik.

Polarization characteristics	Morning (23^h–11^h)		Afternoon (11^h–23^h)	
	Syowa Statinn	Reykjavik	Syowa Station	Reykjavik
Counterclockwise	7	41	20	10
Clockwise	31	0	12	21
Undetermined	3	0	0	1
Total number	41	41	32	32

For the morning pc-5 pulsations, all events are counterclockwise at Reykjavik and 82% of analyzed examples are clockwise at Syowa Station. On the contrary, 63% are counterclockwise at Syowa Station and 68% are clockwise at Reykjavik for the afternoon pc–5 pulsations. These percentages are statistically significant. The average polarization characteristics of pc–5 pulsations are exactly the same as those of *SSC*s described in Chapter III. Namely, the polarization of $\Delta \boldsymbol{H}$ along the line of geomagnetic force is counterclockwise on the morning side (23^h–11^h) and clockwise on the afternoon side (11^h–23^h).

Since the polarization vector is approximately perpendicular to the line of geomagnetic force in all examples, pc–5 pulsations can be interpreted as elliptically polarized transverse hydromagnetic waves.

The above-mentioned results are in perfect agreement with those obtained

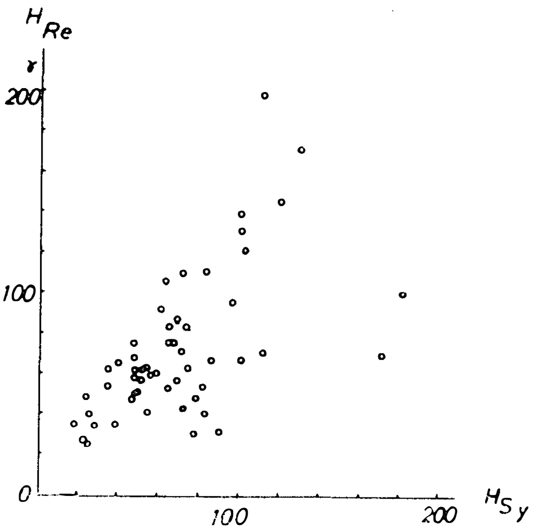

Fig, 5-4. Correlation diagram of amplitude of pc-5 pulsations observed simultaneously at Syowa Station (H_{Sy}) and Reykjavik (H_{Re}).

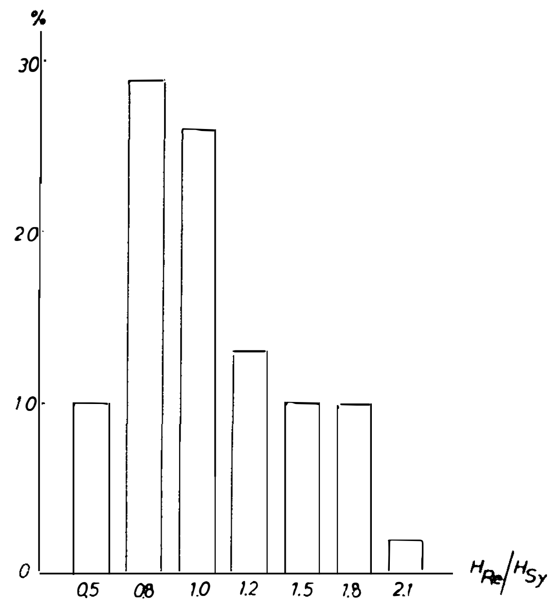

Fig. 5-5. Histogram of ratios of amplitude of pc-5 pulsation at Reykjavik to that at Syowa Station.

by WILSON and SUGIURA (1961), NAGATA *et al.* (1963), WILSON (1963), NAGATA (1964) and KOKUBUN and NAGATA (1965).

From the results of the magnetic measurements by Explorer XII, PATEL (1964) has found that the magnetic pulsations of 100–200 seconds in period observed in the magnetosphere near the equatorial plane are polarized, along the direction of the line of magnetic force, counterclockwise before 11^h in local geomagnetic time and clockwise after 11^h, and that the senses of rotation of magnetic perturbations were coincident with those simultaneously observed at College, Alaska. The other earlier works (JUDGE and COLEMAN, 1962; CAHILL and PATEL, 1963) on the same problem have reached the same conclusion. Thus, the polarization characteristics, their geomagnetic conjugacy and their dependency on local time of pc-5 pulsations and *SSC*s seem to be almost certainly established.

The correlation of the amplitudes of simultaneous pc-5 pulsations between Syowa Station and Reykjavik is illustrated in the correlation diagram of Fig. 5-4. A histogram of ratios of mean amplitudes of the main four wave-cycles of each pulsation at Reykjavik to those at Syowa Station, *i.e.* H_{Re}/H_{Sy}, for 53 simultaneous events of pc-5 pulsations, is shown in Fig. 5-5 where the ratio ranges between 0.5 and 2.1, the average value being 1.04. It will be concluded, therefore, that the amplitudes of pc-5 pulsations are approximately the same at the conjugate stations, the maximum discrepancy being expressed by the 2 : 1 ratio of the larger amplitude to the smaller one.

Fig. 5-6 illustrates the local time dependence of amplitudes of pc-5 pulsation

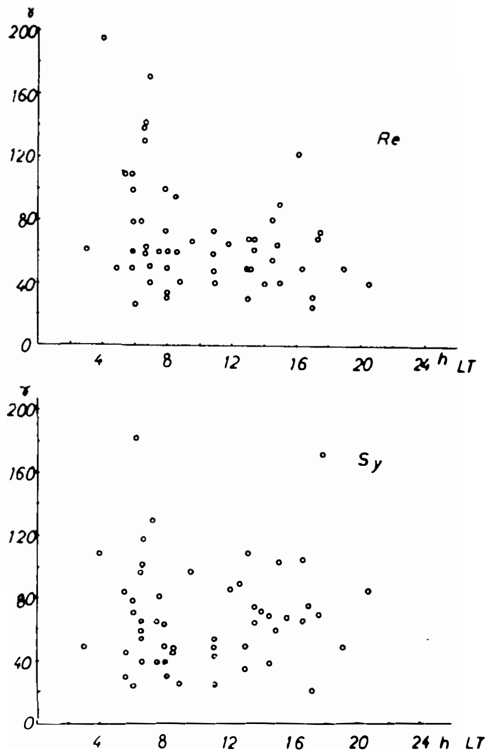

Fig. 5-6. *Dependency of amplitude of pc*-5 *pulsations upon local time at Reykjavik* (*Re*) *and at Syowa Station* (*Sy*).

at the two stations. On the average, the morning pulsations have larger amplitude than the afternoon ones at both stations. However, the above-mentioned dependence on local time is not so much conspicuous in the diagram of Fig. 5–6, where 53 events are plotted altogether. When amplitudes of morning and afternoon pulsations for a period of the same magnitude of polar magnetic disturbances (represented by the same values of K_p index) are compared with each other, then it can be more definitely concluded that the morning pc–5 pulsations are larger than the afternoon ones.

V–4. Frequency spectra of pc-5 pulsations at the conjugate points

In Fig. 5–7, the mean periods of pc–5 pulsations observed at Reykjavik (T_{Re}) are plotted against those observed simultaneously at Syowa Station (T_{Sy}), where the mean periods of pulsations range between 210 sec. and 510 sec. As seen in this diagram, the mean periods of simultaneous pc–5 pulsations are almost exactly the same at the conjugate stations and the absolute majority of the pulsations have a period of 6±1 minutes.

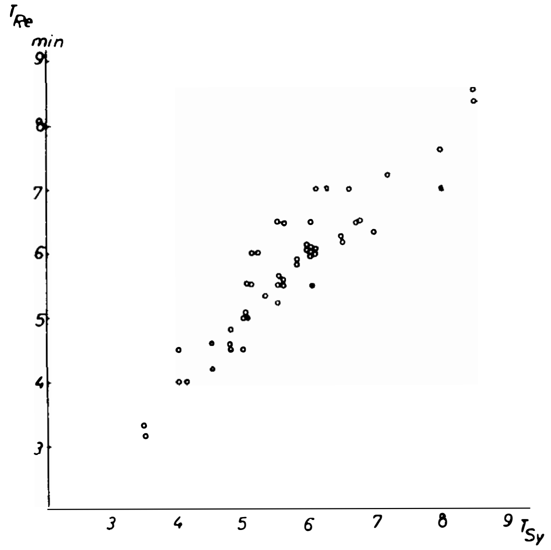

Fig. 5–7. Correlation diagram of period of pc-5 pulsations observed simultaneously at Syowa Station (T_{Sy}) *and Reykjavik* (T_{Re}).

The similarity of the wave form as well as the identity of the mean period of pc–5 pulsations observed simultaneously at the coujugate stations will be examined more precisely based on the frequency spectra of some typical examples of these pulsations. Fig. 5–8 (a), (b), (c) and (d) illustrate the frequency spectra of the morning pulsations at the conjugate stations and Fig. 5–8 (e) and (f) those of the afternoon pulsations. Details of the spectral patterns of these frequency spectra are appreciably dif-

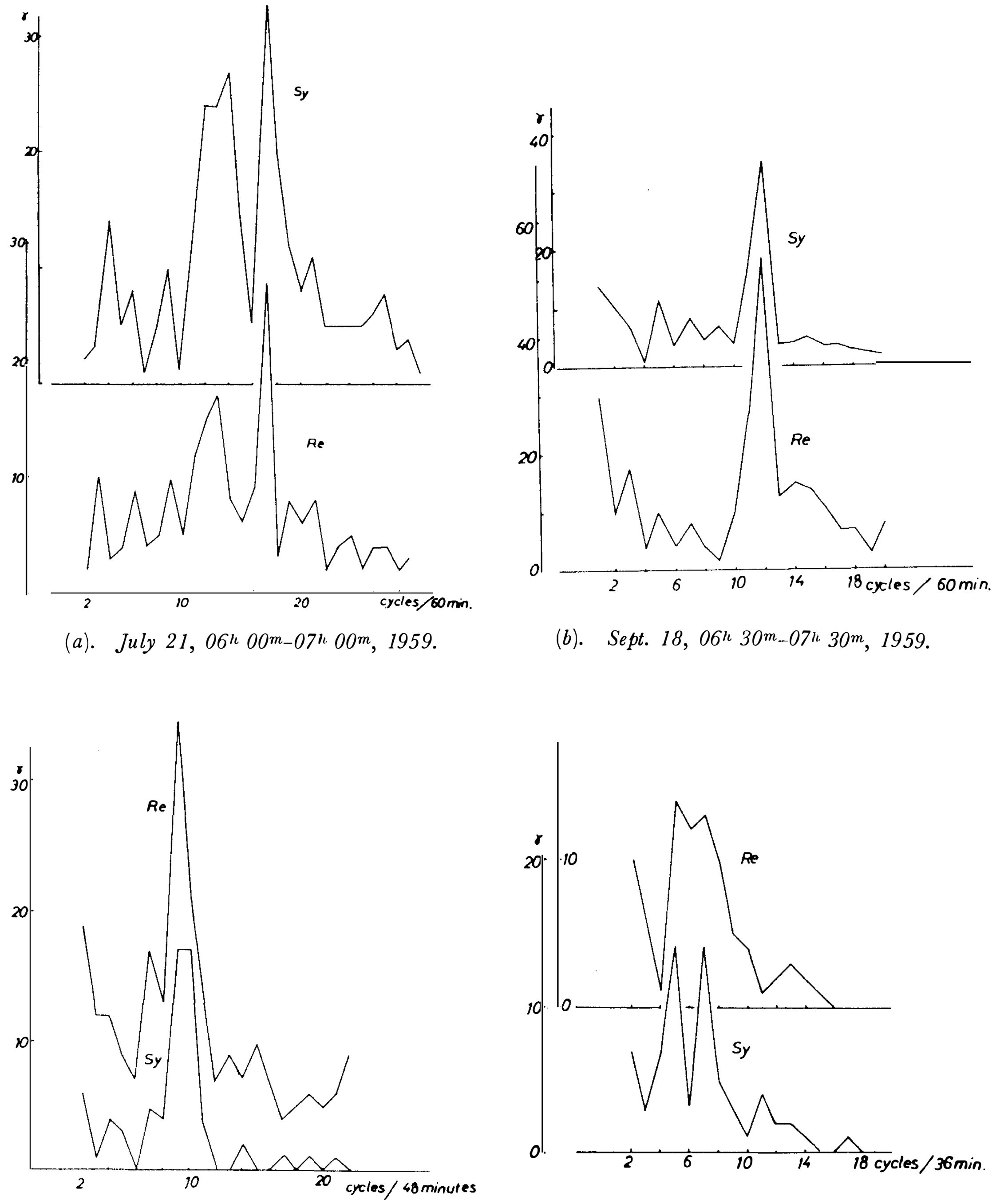

(*a*). *July 21, 06^h 00^m–07^h 00^m, 1959.*

(*b*). *Sept. 18, 06^h 30^m–07^h 30^m, 1959.*

(*c*). *Sept. 5, 06^h 00^m–06^h 48^m, 1959.*

(*d*). *May 9, 03^h 00^m–03^h 36^m, 1959.*

Fig. 5–8. Frequency spectra of pc–5 pulsations observed simultaneously at Syowa Station (Sy) and Reykjavik (Re).

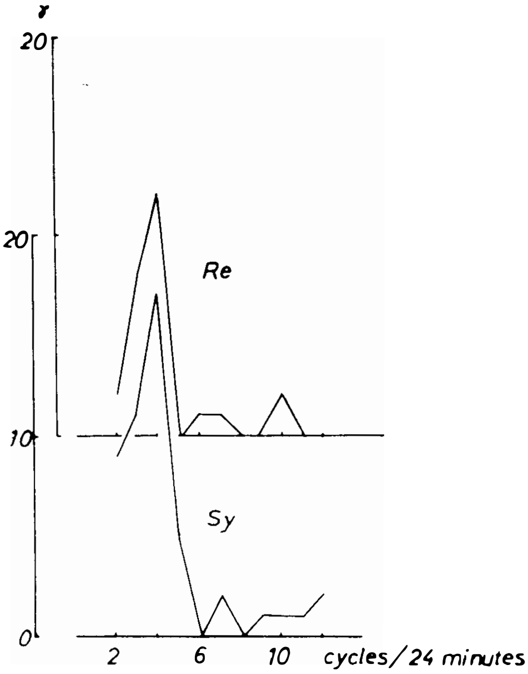

(*e*). *July 26, 13h 06m–13h 03m, 1959.*

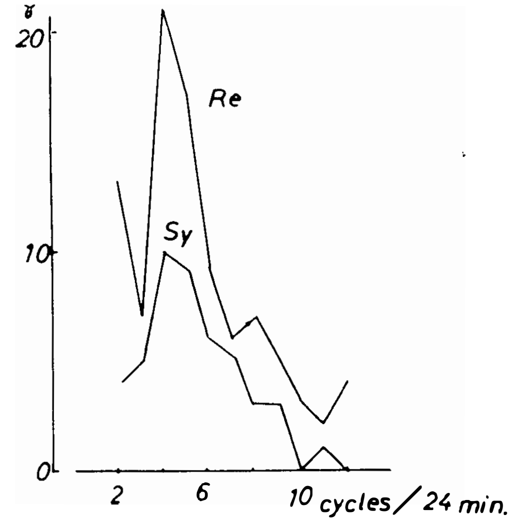

(*f*). *Sept. 19, 16h 30m–16h 54m, 1959.*

ferent from one another at both stations except that their dominant period is 5–6 minutes. When compared with the discrepancy of the frequency spectra between different events, the similarity of the spectra for one event between Syowa Station and Reykjavik is extremely good. For example, the frequency spectra of example (a) have two peaks, at 5.0 min. and 3.5 min., at both stations and their general patterns for the whole range of frequency resemble each other satisfactorily. The most dominant frequency (and the second dominant one in addition when it is not much smaller than the most dominant one) and the *Q*-value for the dominant frequency of those 6 simultaneous examples observed at two stations are sum-

Table V-2. Characteristic parameters of frequency spectra of pc-5 pulsations observed at Syowa Station and Reykjavik.

Examples	Dominant frequency (cps)		*Q*-value	
	Syowa Station	Reykjavik	Syowa Station	Reykjavik
(a)	0.031(0.025)	0.031(0.025)	8.1 (4.7)	8.8 (5.2)
(b)	0.021	0.021	8.4	8.2
(c)	0.021	0.020	5.2	4.5
(d)	0.015(0.021)	0.015(0.021)	3.1 (2.5)	3.0 (2.4)
(e)	0.019	0.019	2.0	2.1
(f)	0.018	0.018	2.0	2.2

Remarks: Figures in parentheses are the values for the second dominant frequency.

marized in Table V-2, where the Q-value is defined, as usual, as

$$Q=2\pi\times\frac{\text{peak energy}}{\text{energy dissipated per cycle}}$$

It is shown in this table that the dominant frequencies are exactly the same and the Q-values also are almost the same at the conjugate stations. Thus, it will be safely concluded that the pc-5 pulsations observed simultaneously at Syowa Station and Reykjavik have almost the same wave structure.

V-5. Some theoretical discussions on generation and propagation of pc-5 pulsations

From all the observed aspects, it seems certain that pc-5 pulsations are transverse hydromagnetic waves generated in the magnetosphere and propagated toward the polar ionosphere of the earth, as suggested by several workers (WILSON and SUGIURA, 1961 ; NAGATA *et al.*, 1963).

As for the general physical parameters of the magnetospheric plasma, we may accept the following figures (CAHILL and MACDONALD, 1964):

Particle density: 5–50 cm^{-3}
Magnetic field: $2\times10^{-4}-2\times10^{-3}$ Gauss
Temperature: $10^{3}-2\times10^{3}$ °K
Mean free path: $1.8\times10^{6}-6.3\times10^{7}$ cm
Lamor radius
  Electron: $5\times10^{2}-7\times10^{3}$ cm
  Proton: $2\times10^{4}-3\times10^{5}$ cm
Gyrofrequency
  Electron (ω_e): $3.5\times10^{3}-3.5\times10^{4}$ sec^{-1}
  Proton (ω_i): $1.9-19$ sec^{-1}
Alfvén velocity (V_A): $6.1\times10^{6}-2.0\times10^{7}$ cm/sec
Sound velocity (V_S): $3.6\times10^{5}-5.1\times10^{5}$ cm/sec

It is concluded, therefore, that $V_A \gg V_S$ in the earth's magnetosphere. Since the dominant frequencies (ω) of pc-5 pulsations range between 0.01 and 0.04 cycle/sec, obviously $\omega \ll \omega_i$ in the magnetospheric plasma. Under these conditions, theoretically possible modes of hydromagnetic waves in the magnetosphere are limitedly

(a) fast magnetoacoustic wave (isotropic wave),

and

(b) slow Alfvén wave (anisotropic wave).

As is known well, the anisotropic wave propagates with $V_A \cos\theta$ in velocity along the direction at an angle θ with the line of magnetic force, and its polarized wave rotates counterclockwise along the direction of the line of magnetic force. On the other hand, the isotropic wave progratës with isotropic velocity (V_A) and its polarization rotates clockwise along the direction of the line of magnetic force.

In regard to the sense of rotation of polarization, therefore, the morning pc-

5 pulsations correspond to the anisotropic wave while the afternoon ones to the isotropic wave (NAGATA *et al.*, 1963). If the initial disturbances in the source are of the same order of magnitude, the amplitude of the anisotropic wave arriving at the ionosphere through the lines of geomagnetic force ought to be larger than that of the isotropic wave, because the wave energy of the former is confined to the direction of the line of magnetic force while the latter propagates isotropically. This theoretical result may explain the observed larger amplitude of morning pulsations as compared with the afternoon ones.

Since $\omega \ll \omega_i$ in the present case, the hydromagnetic waves in the earth's magnetosphere can be approximated by vibrations of the line of magnetic force with damping rate expressed in the term of the Q-value.

Putting F: amplitude of external force

ω: frequency of external force

ω_0: eigen-frequency of the vibrating system

m: mass of the vibrating system

Q: damping rate,

the oscillating perturbation (u) of the vibrating system is expressed as

$$u = Re \left[\frac{\left(\frac{F}{m}\right) e^{j\omega t}}{\omega_0^2 - \omega^2 + j\left(\frac{\omega\omega_0}{Q}\right)} + Ae^{-\omega\left(\frac{t-t_0}{2Q}\right)} e^{j\omega_0\sqrt{1-\left(\frac{1}{2Q}\right)^2}(t-t_0)} \right],$$

where Re denotes the real part of the quantity within the parenthesis. According to the condition, $\omega < \omega_0$, $\omega \approx \omega_0$, $\omega = \omega_0$ or $\omega > \omega_0$, the resultant wave form of u is schematically expressed in Fig. 5–9. Looking through all examples of the observed pc–5 pulsations, such as illustrated in Fig. 5–1, it seems likely that all wave forms shown in Fig. 5–9 can be observed as pc–5 pulsations at the auroral zone stations, but the occurrence frequency of the wave form corresponding to the case of $\omega \approx \omega_0$ is absolutely dominant. This means that a fairly good resonance of ω with ω_0 is taking place in most cases of pc–5 pulsations. Actually the estimated Q-value for pc–5 pulsations, being 2.0–8.5 in Table V–1, indicates that one-half width of the resonance amounts to 0.1–0.5, suggesting a fairly good degree of resonance phenomenon.

From the above-mentioned simple model, it may be concluded that the absolute majority of pc–5 pulsations observed at Syowa Station and Reykjavik are ascribed to the low frequency hydromagnetic wave ($\omega \ll \omega_i$), almost resonating

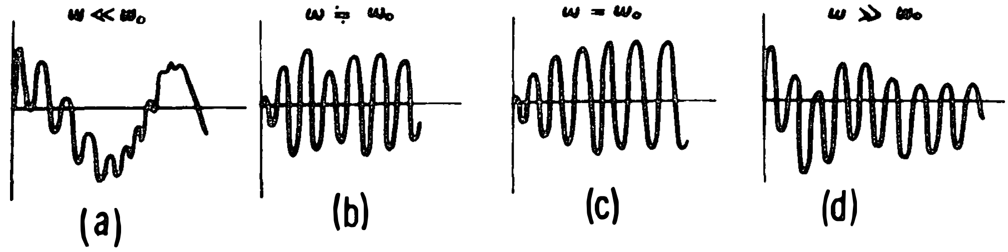

Fig. 5–9. Wave forms of vibration of geomagnetic force.

with the eigen-oscillation of geomagnetic line of force in the magnetospheric plasma.

Since the physical nature of the anisotropic wave is torsional whereas that of the isotropic wave is compressive, the possible external force exciting these waves will be torsional and compressive respectively. Then, it seems possible that the counterclockwise rotating anisotropic wave would be specifically enhanced on the morning side magnetosphere, because the shearing force introduced by the solar wind into the magnetosphere through viscouslike coupling through the magnetopause has the direction to agitate the anisotropic wave on the morning side, whereas it has the direction to suppress the anisotropic wave on the afternoon side.

Then, it would be suggested that the originally dominant cause of generation of pc–5 pulsations is generally of the mode of compression, and a smaller portion of torsional mode is energized specifically on the morning side within the magnetosphere.

As both the isotropic and anisotropic waves can exist in the collisionless plasma in a magnetic field (because $\omega \ll \omega_i$), the dissipation of wave energy during its propagation may be caused mostly through the dynamical damping expressed in the term of the Q-value. Hence, the loss of energy of pc–5 pulsations within the magnetosphere can be estimated using the observed Q-value.

Based on the well-known simple concept of dissipation of wave energy, the rate of energy loss ($\mathcal{E}$) from the wave energy stored in a unit volume (E) is expressed (SLATER and FLANK, 1947) as

$$\mathcal{E}=\frac{\omega}{Q}E$$

Assuming that the kinetic energy of plasma particles is equivalent to the magnetic field energy for the hydromagnetic wave concerned, E is given as

$$E=\frac{1}{8\pi}(\Delta B_0)^2$$

where ΔB_0 denotes the amplitude of hydromagnetic wave of Alfvén mode.

Taking then $Q=5$, T (average period of pulsation) $=300$ sec. and $\Delta B=100\gamma$, we get

$$\mathcal{E}=1.6\times10^{-10}\ \text{erg/cm}^3\ \text{sec.}$$

If we assume that the activated area of pc–5 pulsations, which is generally concentrated within a part of the auroral zone, is 10° wide in latitude and 30° long along the latitude circle, the total volume of the space involving pc–5 pulsations amounts to about 10^{28}cm^3, and consequently the total energy loss is estimated at about 1.6×10^{18} erg/sec.

On the other hand, the average solar wind of 500 km/sec in velocity and 3 proton-electron/cm^3 in number density gives the energy flux of 0.4 erg/cm^2 sec. upon a unit area of the magnetopause. Since the radius of the geomagnetic cavity is about 10 earth's radii, the total energy given by the solar wind to the magnetosphere is estimated at about 1.8×10^{20} erg/sec. It will be thus concluded that about one percent of the wind energy is spent for pc–5 pulsations in the magnetosphere.

General Concluding Remarks

The simultaneity and similarity of three different kinds of geomagnetic disturbances at geomagnetically conjugate points are derived from the present work.

(A) The first kind of phenomenon which is subject to the geomagnetic conjugacy is represented by the auroral electrojet, which takes place simultaneously and in almost the same form at conjugate areas in the northern and southern auroral zones. This phenomenon can certainly be ascribed to simultaneous impinging of corpuscular streams of nearly the same energy spectrum and flux into the north and south auroral zones along the same line of geomagnetic force. A breakup of a reservoir system of electrons (probably accompanied by protons) may result in simultaneous flows of these charged corpuscles both northward and southward along the lines of geomagnetic force passing through the reservoir. In such a case, the energy spectra of impinging corpuscular streams in the conjugate areas specified by the lines of force should be roughly equal to each other. Then, auroral displays, anomalous ionization of the lower ionosphere and resultant auroral electrojet will take place almost simultaneously in the conjugate areas. The observed facts show that the absolute magnitudes of simultaneous auroral electrojets in the conjugate areas are of the same order, the maximum discrepancy between the conjugate electrojets amounting to about two in factor, and that the mode of change in the intensity of electrojet with time is approximately parallel between the conjugate areas. The intensity and its change with time of auroral electrojet are approximately proportional to the flux and its change with time of impinging corpuscular stream. Then, a possible mechanism of emitting corpuscular streams from the reservoir will be fairly symmetric with respect to the geomagnetic equatorial plane. In other words, mechanism of corpuscular emission may be due to something like a systematic change in the pitch angle of corpuscles caused by a change in the magnetic field intensity in the corpuscular reservoir in the outer space or systematic accerelation of corpuscular energy component parallel to the line of force by appreciable change in the lateral gradient of the field, etc.

(B) The second kind of phenomenon subject to the geomagnetic conjugacy is the low frequency hydromagnetic wave represented by pc-5 pulsations, *SSC*s and *SI*s. As described in Chapters III, IV and V, these three phenomena have common characteristics of their polarization; counterclockwise polarization along the line of geomagnetic force (*i. e.* lefthand polarization) on the morning side and clockwise polarization (*i.e.* righthand polarization) on the afternoon side. Since the frequency (ω) of these geomagnetic variations are much smaller than the ion gyrofrequency (ω_i) in the space concerned, those magnetic variations seem to be identified as the two kinds of low frequency hydromagnetic waves of Alfvén mode, *i.e.*, the fast wave of Alfvén mode having the righthand polarizataion (isotropic wave) and the slow wave of Alfvén mode having the lefthand polarization (anisotropic wave).

If the observed waves are of pure Alfvén mode, their polarization viewed along the lines of magnetic force should be circular. However, the observed polarization of pc–5 pulsations, *SSC*s and *SI*s are always elliptic even in the auroral zones where the amplitude of pc–5 pulsations takes the maximum value.

Therefore, the simultaneous pc–5 pulsation having the same frequncy spectra as observed at the conjugate areas, such as Syowa Station and Reykjavik, may not be directly identified as the transverse hydromagnetic waves propagating just along a line of geomagnetic force passing through these conjugate points in the magnetospheric plasma. Possible refraction through the ionosphere, where the hydromagnetic waves are transformed into the electromagnetic waves in the nonionized medium, and possible effect of curvature and gradient of the lines of magnetic force may have to be taken into account in theoretical interpretation of the observed phenomena in more detail.

One of the main difficulties involved in the theoretical interpretation discussed in Chapter V will be concerned with a fact that pc–5 pulsations having clockwise polarization on the afternoon side also take the maximum amplitude in the auroral zones. This observed fact may indicate that the energy of hydromagnetic wave of this kind also is confined mostly to the specified tubes of geomagnetic force passing the auroral zones. If the pulsation of clockwise polarization is identfied as the fast wave of pure Alfvén mode (isotropic wave) having clockwise polarization, such an observed concentration of wave energy cannot be directly expected. It will be obvious, however, that the distribution of Alfvén velocity is not homogeneous in the magnetosphere. Based on the hydromagnetic ray theory which is valid as an approximate representation of hydromagnetic waves of Alfvén mode, Sugiura (1964) examined the propagation of the isotropic Alfvén wave in the magnetosphere. According to him, the earth and its immediate vicinity are well protected from the hydromagnetic rays generated in the outer region of the magnetosphere, because the barrier of the maximum Alfvén velocity located several thousand kilometers above the earth's surface tends to reflect the hydromagnetic rays coming from the outer magnetosphere where the Alfvén velocity decreases with increasing geocentric distance. Only when the initial direction of the rays deviated from the meridian plane by a small angle, they can reach the earth's vicinity except directly above the poles. Hence, it would be theoretically expected that the isotropic Alfvén wave can hardly arrive at the polar cap areas.

On the other hand, the damping of hydromagnetic waves in the plasma with appreciable collision in the lower region of magnetosphere is much less along the lines of magnetic force than perpendicularly to the lines. The propagation distance (the distance for damping down to 1/e) of Alfvén waves is proportional to the electric conductivity along the direction concerned (KAHALAS, 1960). Since the conductivity $\sigma_{\parallel}$ along the line is much larger than the conductinity $\sigma_{\perp}$ perpendicular to the line in the lower magnetosphere, the isotropic Alfvén waves propagating to the ionospheric level in temperate and low latitudes must be remarkably damped as compared with those propagating to high latitudes.

It seems likely that the observed dependency on latitude of pc–5 pulsations of clockwise polarization is qualitatively ascribed to the above-mentioned two factors. However, a more exact theoretical approach to this problem, based on the wave theory of hydromagnetic waves in inhomogeneous anisotropic media, will be highly necessary.

(C) The third kind of phenomenon subject to the geomagnetic conjugacy is the electric charge transfer from the outer magnetosphere along the line of geomagnetic force to the earth's polar ionospheric regions, such as S_q^p field and the SP-component of D_p polar magnetic field. If we accept the concept of a magnetospheric dynamo which is composed of general circulation of the low energy plasma and the geomagnetic field in the outer magnetosphere, then the electric field produced by such a dynamo in and near the geomagnetic equatorial plane will be transferred along the high conductive line of force approximately equally to the ionosphere regions of the conjugate areas, resulting in the S_q^p-like ionospheric current patterns in both polar regions.

The observed remarkable seasonal variation of the S_q^p field has been reasonably attributed to the seasonal change in the ionospheric conductivity. If the SP-component of a polar magnetic storm (D_p field) is interpreted as an intensified S_q^p field, the intensity of the SP field also ought to have an appreciable seasonal variation. As this key point is not examined in the present work, future critical researches on this particular point are desired.

References

ALFVÉN, H. and C. G. FÄLTHAMMAR: Cosmical electrodynamics, Second edition, Oxford Univ. Press, 1963.

AXFORD, W. I. and C. O. HINES: A unifying theory of high latitude geophysical phenomena and geomagnetic storms. Can. J. Phys., **39**, 1433, 1961.

BOSTRÖM, R.: A model of the auroral electrojets. J. Geophys. Res., **69**, 499, 1964.

CHAPMAN, S.: Earth storms; Reprospect and prospect. J. Phys. Soc. Japan, **12**, Suppl, A-I, 6, 1962.

CHAMBERLAIN, J. W.: Theory of auroral bombardment. Astrophys. J., **134**, 401, 1961.

COLE, K. D.: A dynamo theory of the aurora and magnetic disturbance. Austral. J. Phys., **13**, 484, 1960.

COLE, K.D.: A note on partial criticisms of dynamo theory of magnetic disturbance. J. Atmospheric Terr. Phys. **24**, 541, 1962.

DENISSE, J. E. and J. L. DELCROIX.: 'Plasma waves', Interscience Tracts on Physics and Astronomy, No. 17, 1963.

FEJER. J. A.: Hydromagnetic wave propagation in the ionosphere. J. Atmospheric Terr. Phys., **18**, 135. 1960.

FEJER, J. A.: Theory of auroral electrojet. J. Geophys. Res., **68**, 2147, 1963.

FEJER, J. A.: Theory of geomagnetic daily disturbance variations. J. Geophys. Res., **29**, 123, 1964.

FRANCIS, W. E. and R. KARPLAS: Hydromagnetic waves in the ionosphere. J. Geophys. Res., **65**, 3593, 1960.

HAKURA, Y.: Tables and maps of geomagnetic coordinates corrected by the higher order spherical harmonic terms. Rep. Ionosphere Space Res. Japan, **19**, 121, 1965.

JUDGE, D. L. and P. J. COLEMAN, Jr.: Observations of low-frequency hydromagnetic waves in the distant geomagnetic field: Explorer 6. J. Geophys. Res., **62**, 5075, 1962.

KAHALAS, S. L.: Magnetohydrodynamic wave propagation in the ionosphere. Phys. Fluid, **3**, 372, 1960.

KERN, J. W.: A charge separation mechanism for the production of polar aurora and electrojets. J. Geophys. Res., **67**, 2649, 1962.

KOKUBUN, S.: Dynamic behaviour and north-south conjugacy of geomagnetic bays. Rep. Ionosphere Space Res. Japan, **19**, 177, 1965.

KOKUBUN, S. and T. NAGATA: Geomagnetic pulsations (pc-5) in and near the auroral zones. Rep. Icnosphere Space Res. Japan, **19**, 158 1965.

LINHART, J. G.: 'Plasma Physics'. North Holland Publishing Company, Amsterdam, 1960.

MACDONALD, G. J. F.: Hydromagnetic waves in space. 'Space Research', 474, John Wiley & Sons, Inc., New York, 1964.

MATSUSHITA, S.: On geomagnetic sudden commencements, sudden impulses, and storm durations. J. Geophys. Res., **67**, 3753, 1962.

MEAD, G. D.: Deformation of the geomagnetic field by the solar wind. J. Geophys. Res, **69**, 1181, 1964.

NAGATA, T. and H. ONO: Developmant of SD-field with storm-time. J. Geomag. **4**, 108, 1952.

NAGATA, T. and N. FUKUSHIMA: Constitution of polar magnetic storms. Rep. Ionosphere Res. Japan, **6**, 85, 1952.

NAGATA, T. and N. FUKUSHIMA: Characteristics of polar magnetic storms. Indian J. Meteor.

Geophys., **5**, 75, 1954.

NAGATA, T. and S. ABE: Note on the distribution of SC* in high latitude. Rept. Ionosphere Res. Japan, **9**, 39, 1955.

NAGATA, T. and S. KOKUBUN: Polar magnetic storms, with special reference to relation between geomagnetic disturbances in the northern and southern auroral zones. Rep. Ionosphere Space Res. Japan, **14**, 273, 1960.

NAGATA, T. and S. KOKUBUN: A particular geomagnetic daily variation ($S_q{}^p$) in the polar regions on geomagnetically quiet days. Nature, **195**, 555, 1962.

NAGATA, T. and S, KOKUBUN: An additional geomagnetic daily variation field ($S_q{}^p$-field) in the polar region on geomagnetically quiet days. Rep. Ionosphere Space Res. Japan, **16**, 256, 1962.

NAGATA, T.: Morphology and some interpretation of geomagnetic variations in Antarctica, Antarctica Research. Geophys. Monograph. No. 7, American Geophys. Union, 89, 1962.

NAGATA, T., S. KOKUBUN and T. IIJIMA: Geomagnetically conjugate relationships of giant pulsations at Syowa Base, Antarctica, and Reykjavik, Iceland. J. Geophy. Res., **68**, 4621, 1963.

NAGATA, T.: Polar geomagnetic disturbances. Planet. Space Sci., **11**, 1395, 1963.

NAGATA, T., and T. IIJIMA: Simultaneous current patterns of polar magnetic storms (D_p-field) in the northern and southern polar regions during IGY. J. Geomag. Geoele., **16**, 210, 1964.

NAGATA, T.: Magnetic field at the poles. Research in geophysics. part I, 423, MIT press, 1964.

NISHIDA, A, and J. A. JACOBS: World-wide changes in the geomagnetic field. J. Geophys. Res., **67**, 525, 1962.

NISHIDA, A., and J. H. YOUNG: Explorer XII observations of magnetic sudden impulses in the earth's magnetosphere. Nature, **201**, 1113, 1964.

OBAYASHI, T., and J. A. JACOBS: Sudden commencement of magnetic storms and atmospheric dynamo action. J. Geophys, Res, **62**, 589, 1957.

OGUTI, T.: Notes on the morphology of SC. Rep. Ionosphere Res. Japan, **10**, 81, 1956.

OGUTI, T., and T. NAGATA: Interrelations among the upper atmospheric disturbance phenomena in the auroral zone. Rep. Ionosphere Space Res. Japan, **15**, 31, 1961.

PATEL. V. L., and L. T. CAHILL: Evidence of hydromagnetic waves in the earth's magnetosphere and their propagation to the surface. Phys. Rev. Letters, **12**, 213, 1964.

PIDDINGTON, J. H.: Hydromagnetic waves in ionized gas. Monthly Notices. Roy. Astronom. Soc., **115**, 671, 1955.

PIDDINGTON, J. H.: A theory of polar geomagnetic storms. Geophys. J., **3**, 314, 1960.

PIDDINGTON, J. H.: A hydromagnetic theory of geomagnetic storms. Geophys. J., 183, 1962.

SLATER and FLANK: 'Mechanics'. Mc-Graw Hill, Book Company Inc., 1947.

SPITER, L. Jr.: 'Physics of fully ionized gases', Interscience Publishers, Inc., New York, 1956.

SNYDER, C. W., M. NEUGEBANER and U. R. RAO: The solar wind velocity and its correlation with cosmic ray variations and with solar and geomagnetic activity. J. Geophys. Res., **68**, 6361, 1963.

SUGIURA, M. and S. CHAPMAN: The average morphology of geomagnetic storms with sudden commencements. Abh. Akad. Wiss. Göttingen, Math-phys. KI. Sonderheft, Nr. 4, Göttingen, 1960.

SUGIURA, M.: Evidence of low-frequency hydromagnetic waves in the exosphere, J. Geophys. Res., **66**, 4087, 1961.

SUGIURA, M.: Hourly values of equatorial Dst for the IGY. NASA. Goddard Space Flight Center, Reprint, X-611-63-131, 1962.

SUGIURA, M.: Propagation of hydromagnetic waves in the magnetosphere. NASA, Goddard

Space Flight Center, publication X-611-64-240, 1964.

Stix, T. H.: 'Theory of plasma waves'. Mc-Graw Hill, Book Company Inc, 1964.

Swift, D. W.: The generation and effect of electrostatic fields during an auroral disturbance. J. Geophys. Res., **68**, 2135, 163.

Vestine, E. H.: Note on conjugate point of geomagnetic field line for some selected auroral station of the IGY. J. Geophys. Res., **64**, 1411, 1959.

Vestine, E. H. and W. L. Sibley: Remarks on auroral isochasms. J. Geophys. Res., **64**, 1338. 1959.

Vestine, E. H. and J. W. Kern: Cause of preliminary reverse impulse of storms. J. Geophys. Res., **67**, 2181, 1962.

Vestine, E. H.: Morphology of magnetic storms. J. Phys. Soc. Japan, **17**, Suppl. A-I, 61, 1962.

Wescott, E. M.: Magnetic variations at conjugate points. J. Geophys. Res., **66**, 1789, 1961.

Wescott, E. M.: Magnetic activity during periods of aurora at geomagnetically conjugate points. J. Geophys. Res., 1353, 1962.

Wilson, C. R., and M. Sugiura: Hydromagnetic interpretation of sudden commencements of magnetic storms. J. Geophys. Res., **66**, 4097, 1961.

Wilson, C. R.: Hydromagnetic interpretation of sudden commencements of geomagnetic storms. Geophys. Inst. Univ. of Alaska, Sci. Rept. AECRL-63-605, 1963.

(*Manuscript received December 20, 1965*)